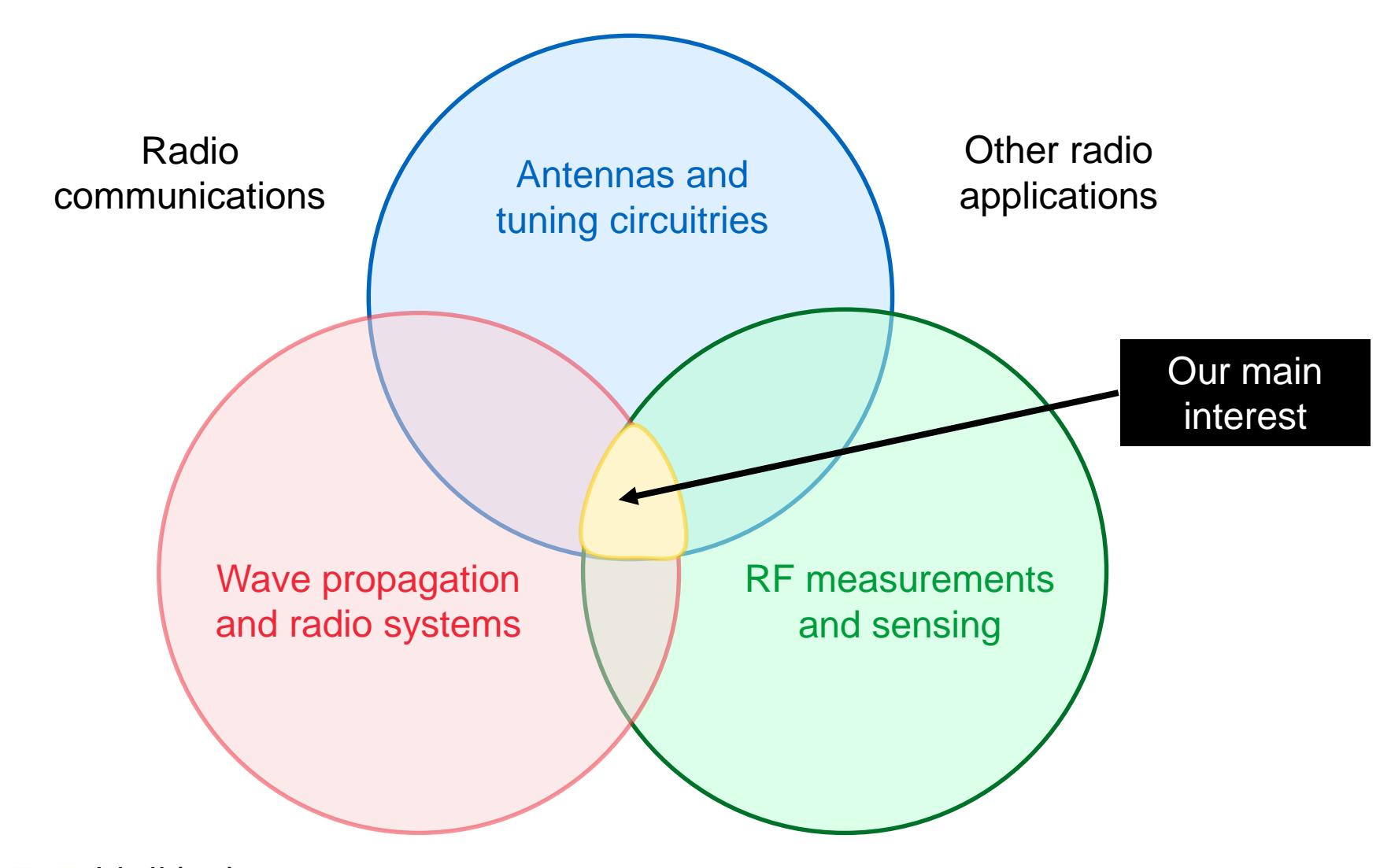


Challenges in Radio Research for Future Generation Wireless Systems

Katsuyuki Haneda (on behalf of RF&MW team members)

Department of Electronics and Nanongineering Aalto University School of Electrical Engineering September 10 2018

Our Competence and Interests





Our Group & Projects Antennas and tuning circuitries Academy/TEKES Academy **Massive MIMO** Full-duplex Mr. Christian Radio Other radio Cziezerski communications applications Mr. Mikko Heino Academy Mm-wave D2D Dr. Aki Karttunen **TEKES** Dr. Clemens **MIMOTA2** H2020 **I**cheln Mr. Pasi Koivumaki mmMagic Mr. Suzan Miah Mr. Usman Virk Wave propagation RF measurements **Aalto University**



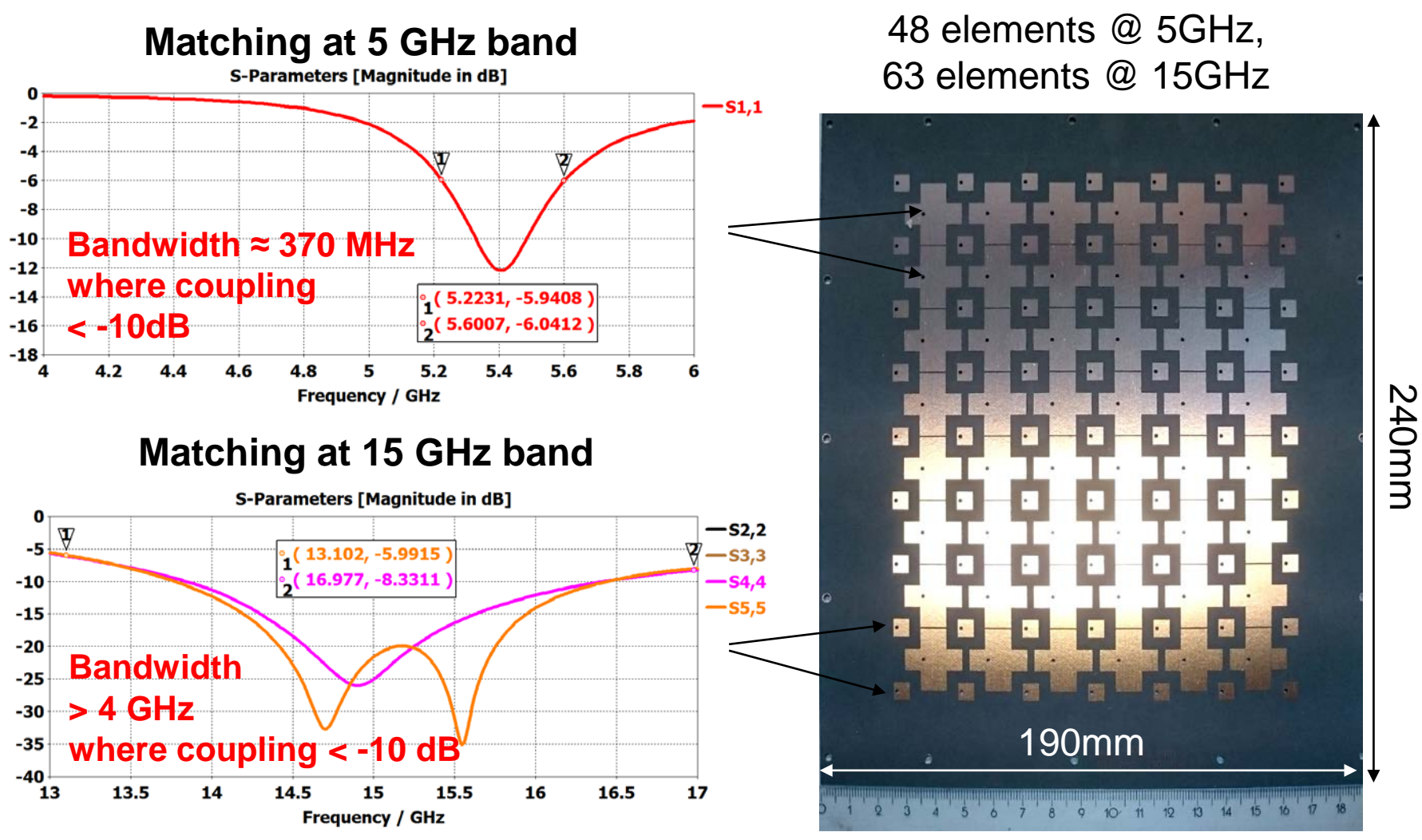
Wave propagation and radio systems

RF measurements and antenna testing

Multiple-Element Antennas and Antenna Decoupling Techniques



Dual-Band Massive Antenna Array for Small-Cell Infrastructure





L. Li and A. Muhammad, PIMRC'16.

28 GHz Phased Antenna Array Module

Antenna under test: ULA based on a Rotman lens

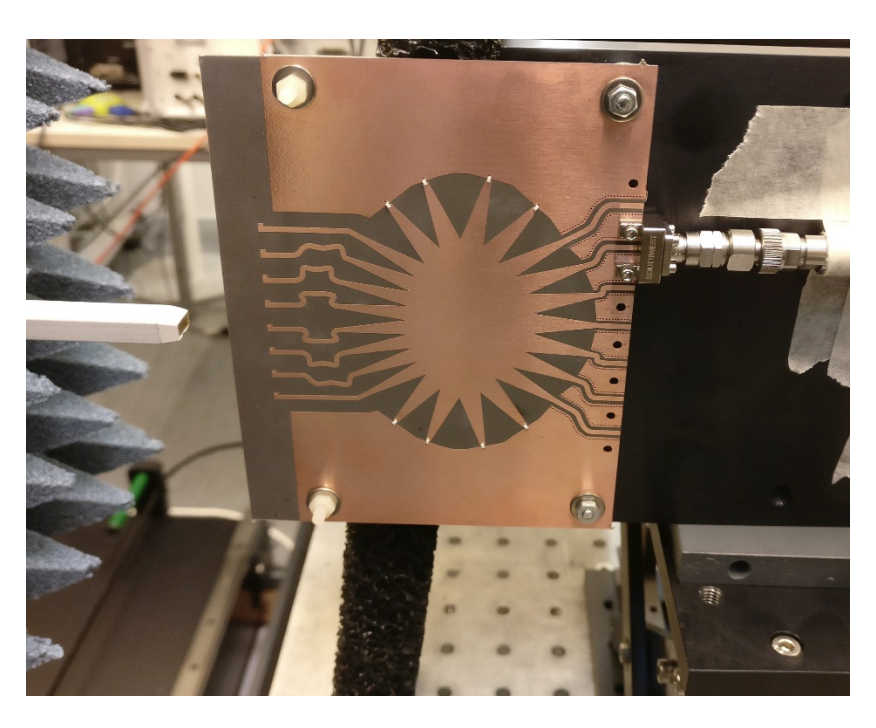


Figure: Rotman lens integrated antenna array measured in near-field radiation pattern measurement system.

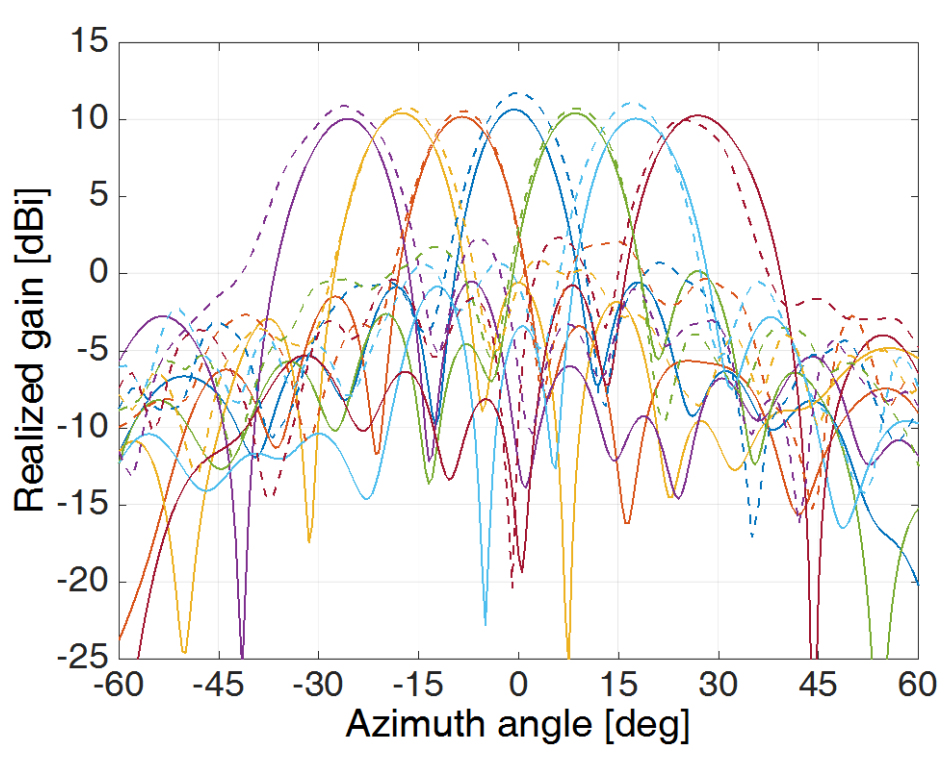
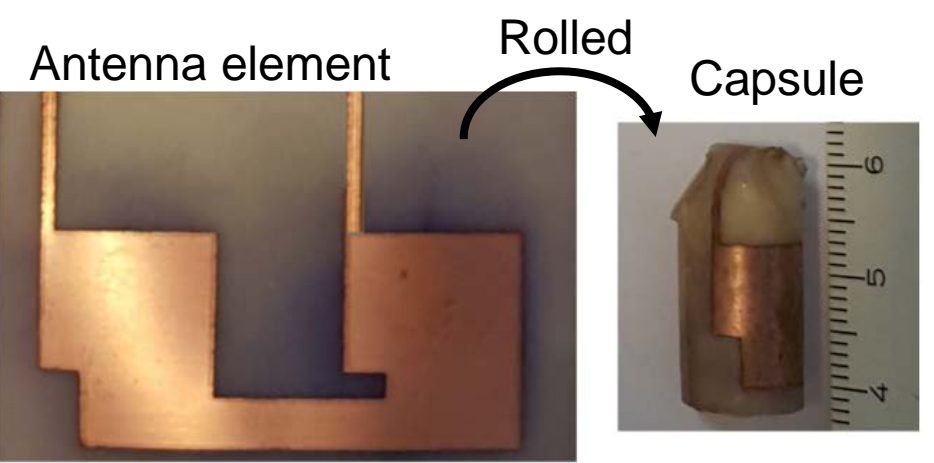


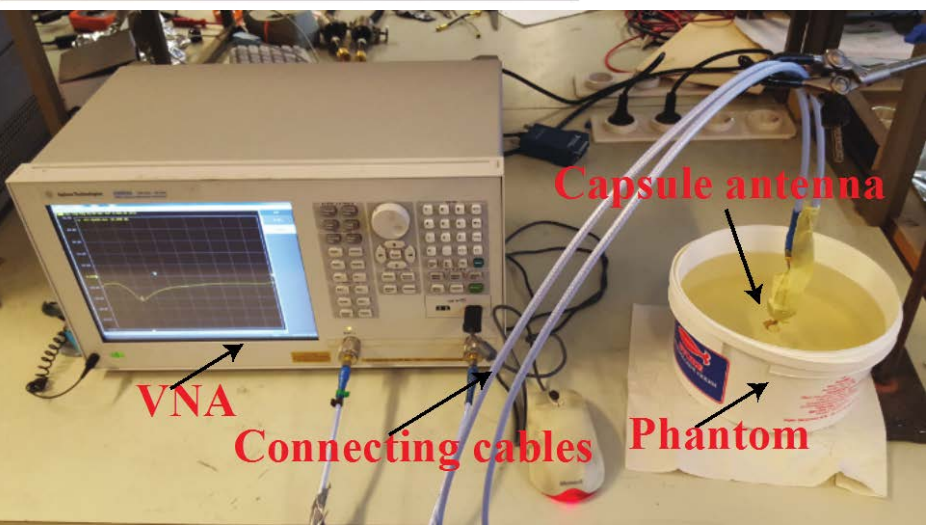
Figure: measured (solid) and simulated (dashed) radiation patterns of the antenna array.

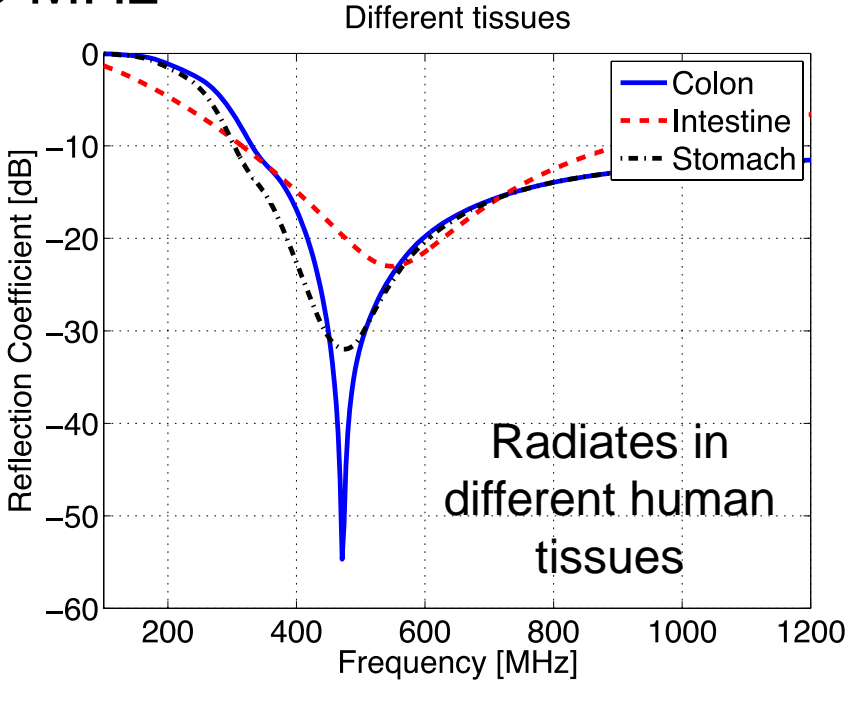


Conformal, Swallowable Capsule Antenna

For wireless endoscope @ 433 MHz





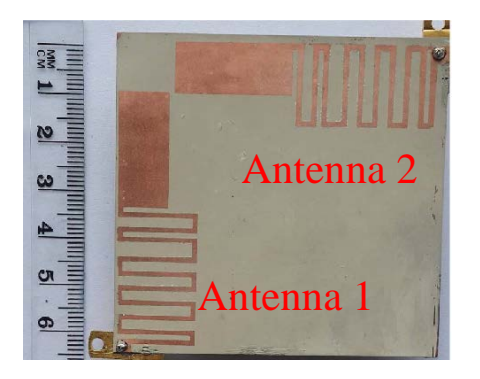


- Simulations and experiments using liquid human phantom showed excellent agreement of matching.
- Detuning due to different human tissues overcome by ultrawideband matching.



Electrically-Small Multi-Element On-Body Antenna

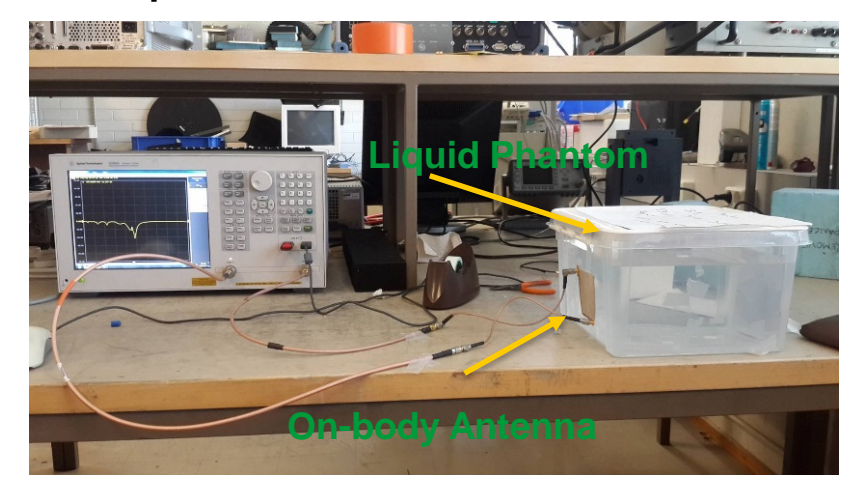
 For a receiver unit of the wireless capsule endoscopy operating at 433 MHz



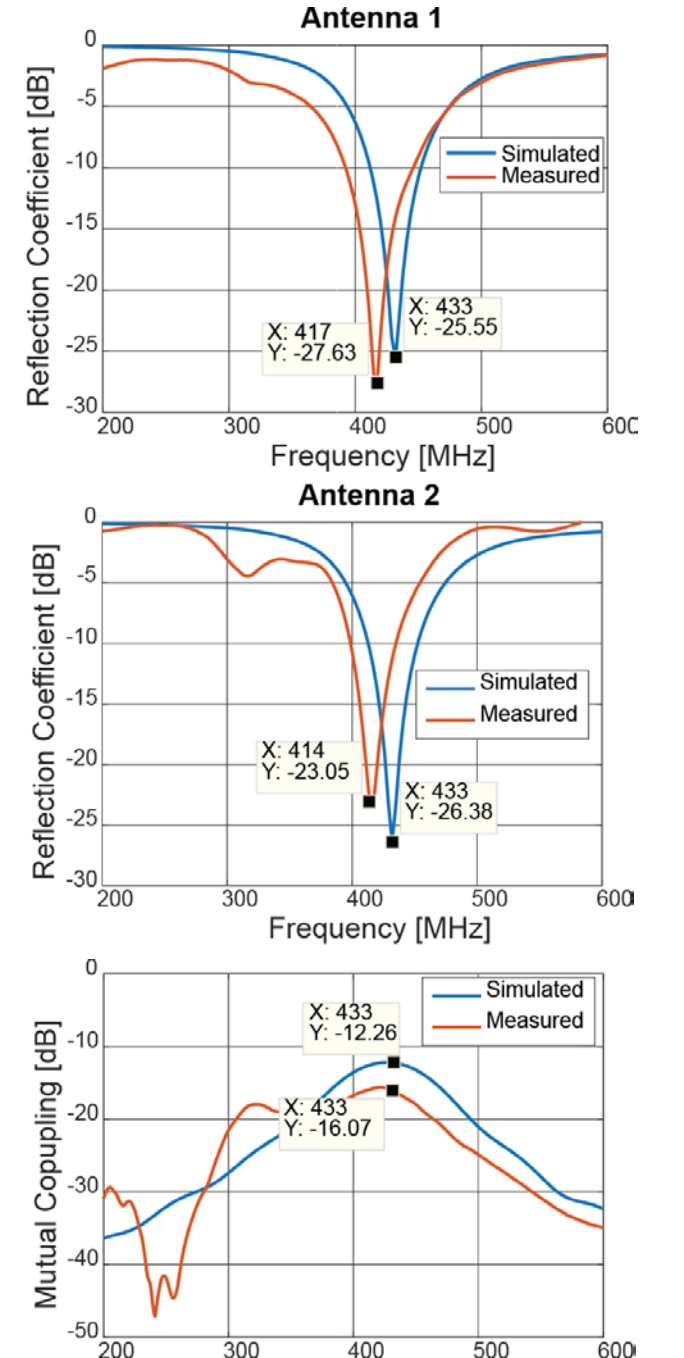
Top View



Back View



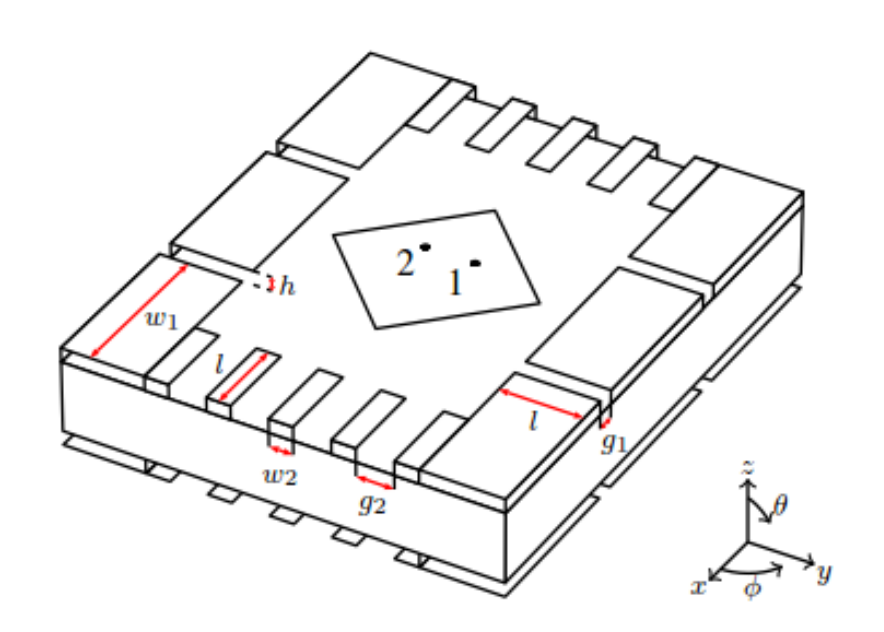
- Simulations and measurements show good agreement.
- Mutual coupling is less than -10 dB in the bandwidth of interest (400-500 MHz).
 A. N. Khan, master's thesis, 2016.

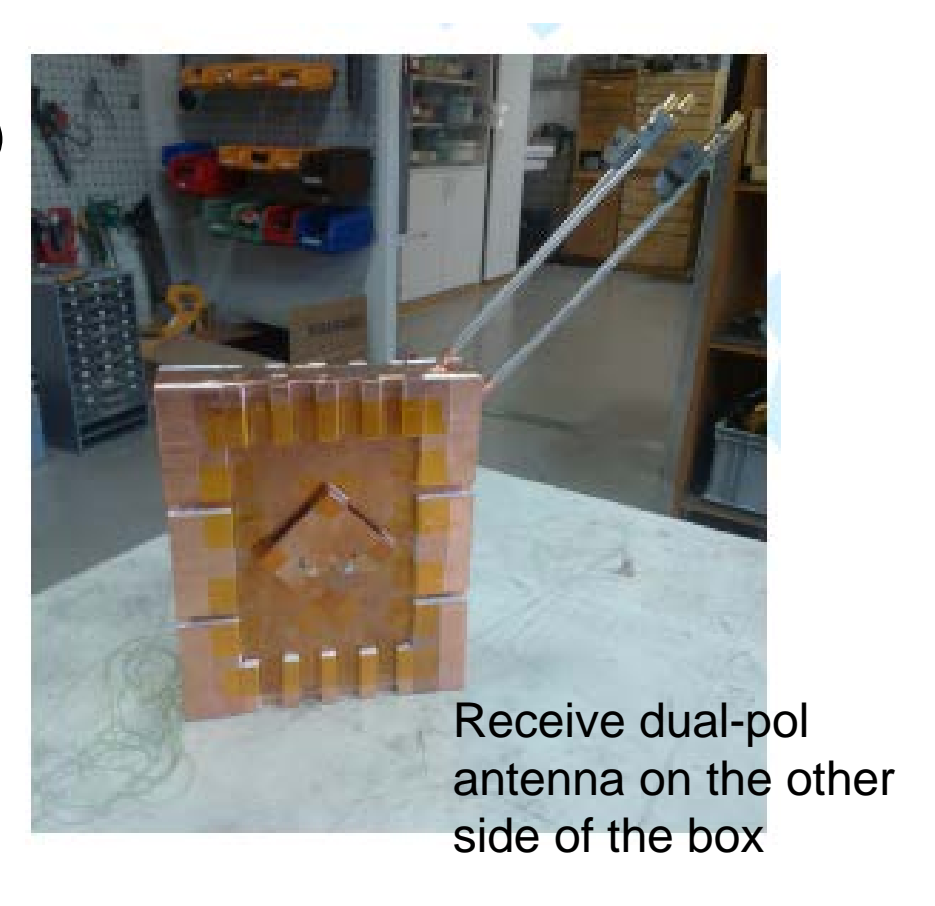


Frequency [MHz]

Wavetraps for Isolation Improvement of In-Band Full-Duplex Relay Antennas

Enable dense antenna placement: Example 1: 2x2 relay (back-to-back) prototype w/dual-polarised patches





M. Heino et al., IEEE Trans. Ant. Prop., 2016.



Wavetraps for Isolation Improvement

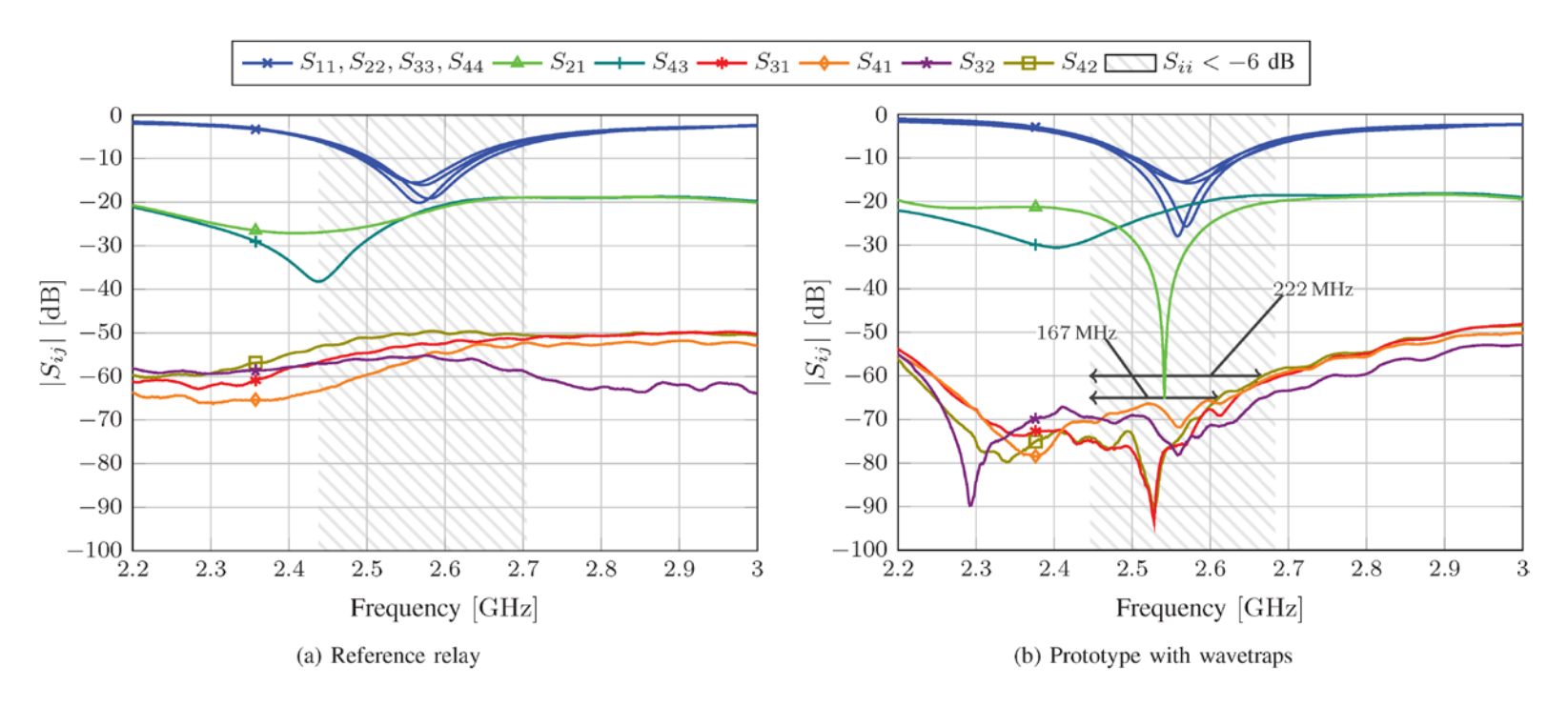


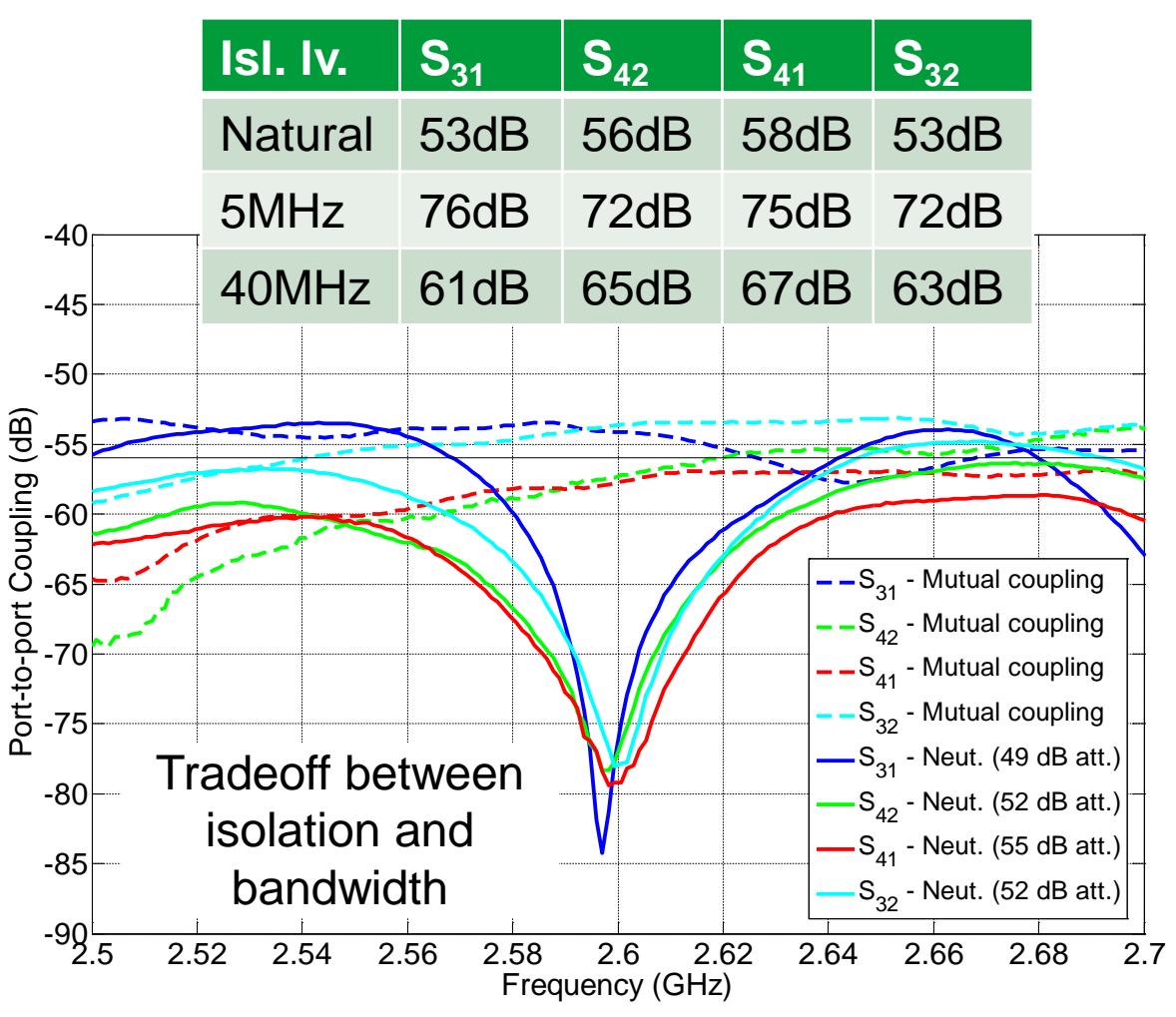
Fig: Measured isolation before (left) and after (right) adding wavetraps

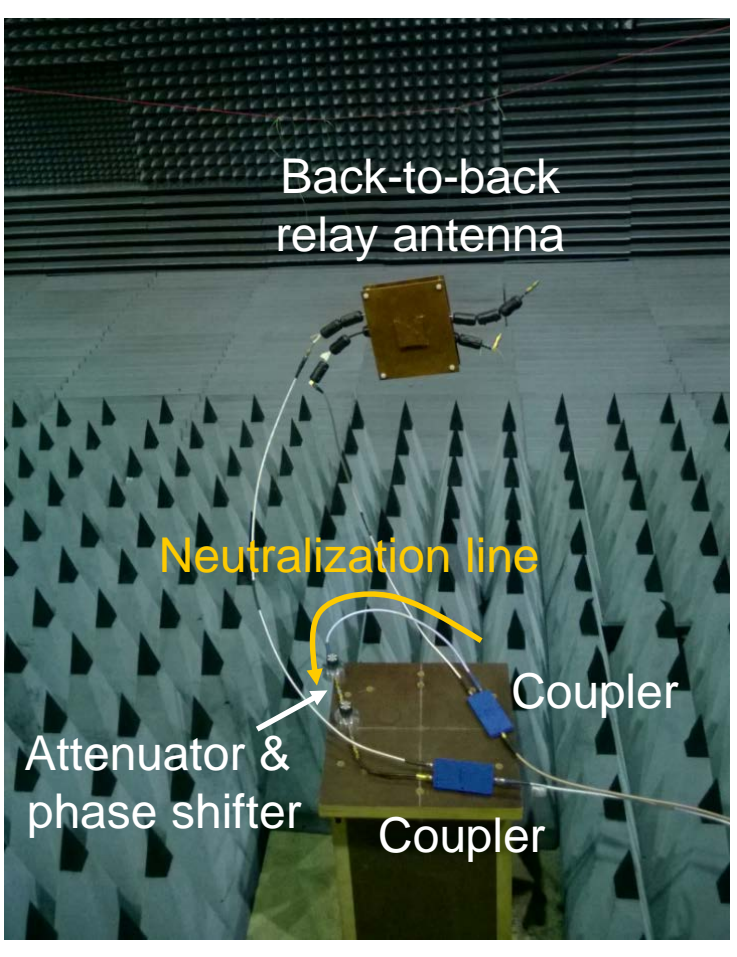
- High isolation (>60 dB) across wide frequency band (9%)
- Can also be applied to co-planar dense patch arrays
- Can be extended to dense arrays above 6 GHz by adjusting the wavetrap shape and size



Passive Antenna Decoupling Circuitry: A Neutralization Line



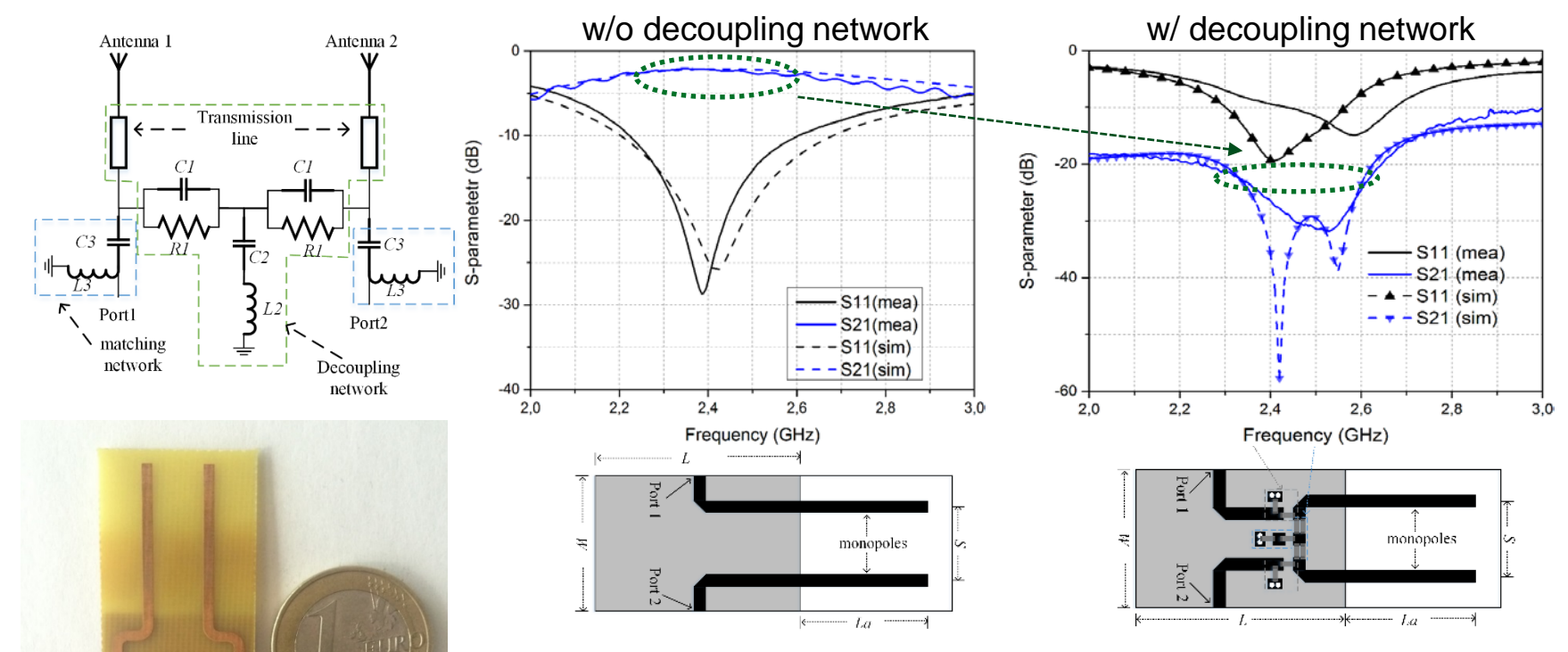






S. Venkatasubramanian *et al.*, EuCAP2015 (finalist of a student paper award).

Wideband Antenna Decoupling Network for a Compact Monopole Array



- More than 15dB isolation improvement in 12% bandwidth
- Can be extended to dense array above 6GHz by replacing lumped components with varactor diodes and microstrip structures.



Wideband Antenna Decoupling Using Resistive

Circuitries

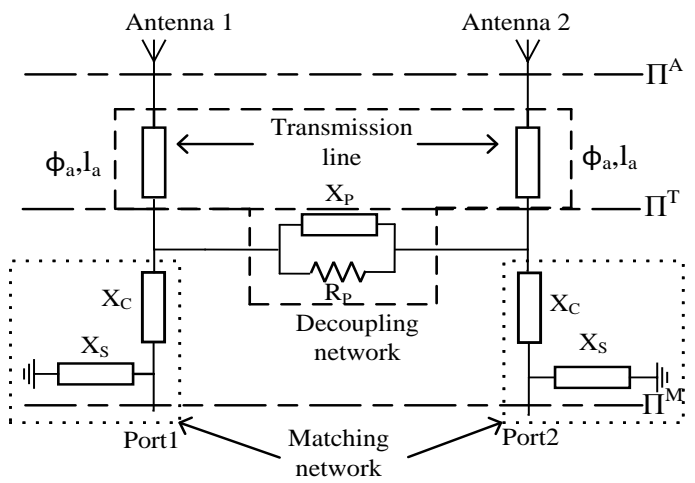


Fig. 1 Decoupling network schematic.

(gp) -10

Building -15

Reference
- - Prototype 1
---Prototype 2
---Prototype 3

Fig. 3 Measured isolation.

2.4

Frequency (GHz)

2.5

2.6

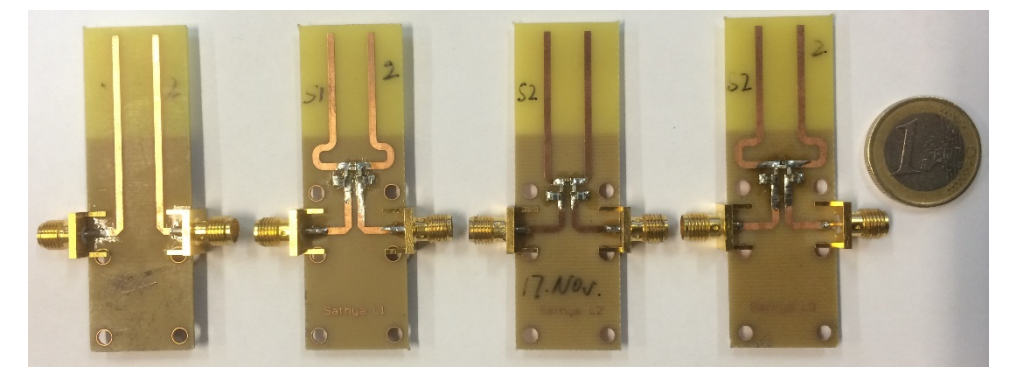


Fig. 2 Prototypes with different decoupling circuits.

- Transmission lines at antenna feeds to transform phase of mutual admittance.
- Resistive and reactive elements connected between antenna feeds to improve wideband isolation

INPUT MATCHING AND ISOLATION BANDWIDTHS OF THE THREE PROTOTYPES AS WELL AS THE REFERENCE DESIGN AROUND 2.4 GHz.

	Match	ing BW (MHz)	Isolation BW (MHz)				
Level	−10 dB		15 dB		20 dB		
	Sim.	Meas.	Sim.	Meas.	Sim.	Meas.	
Reference	475	375	0	0	0	0	
1	290	330	330	370	130	165	
2	270	330	425	455	175	190	
3	220	215	515	500	110	140	



2.3

2.2

Radio Channel Modeling at High Frequencies

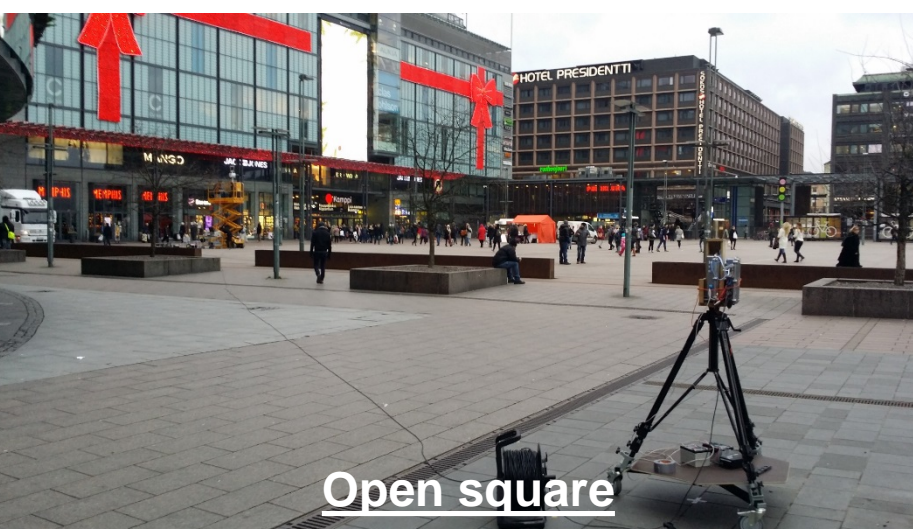


High-Frequency Channel Sounding

 Capable of sounding at <6, 15, 28, 60, 70 and 80 and above 100 GHz



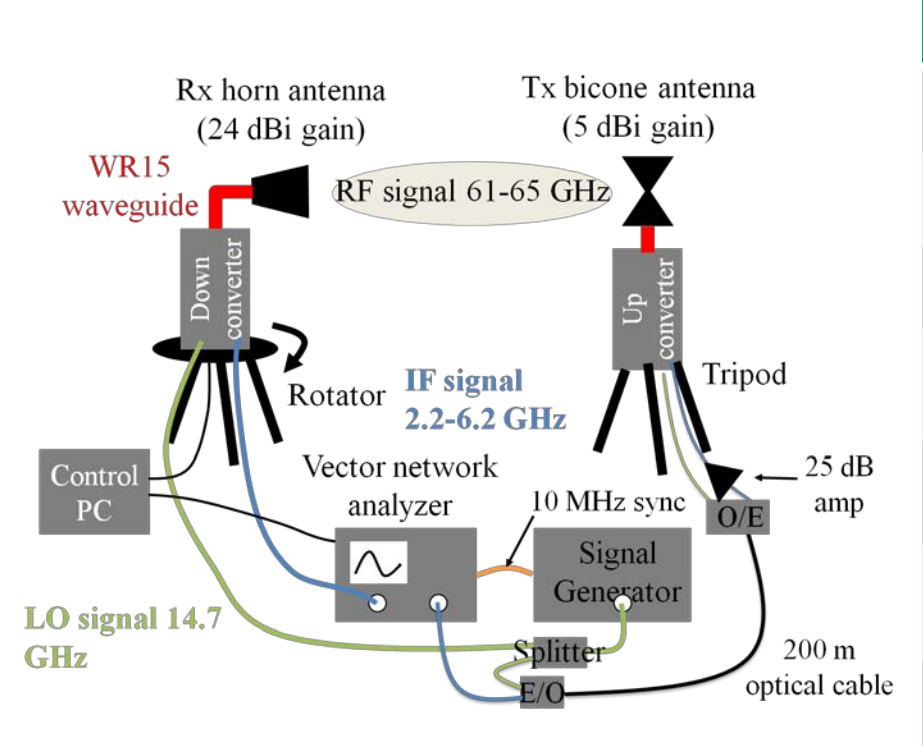












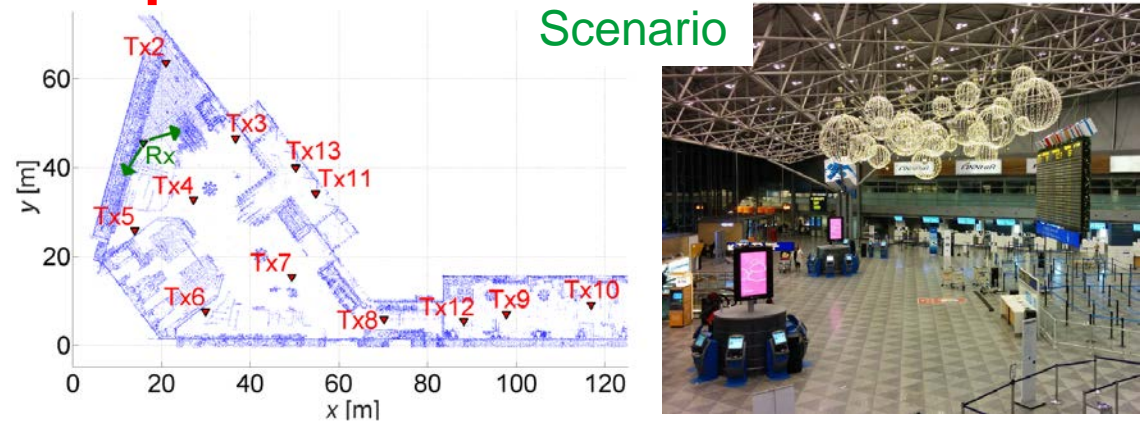
Frequency range	61-65 GHz/ 69-74 GHz	27-30 GHz	14-16 GHz
Bandwidth	4-5 GHz	3 GHz	2 GHz
Freq. sweep points	10001	10001	10001
Multipath resolution	0.2-0.25 ns	0.33 ns	0.5 ns
Max. detectable delay	2000 ns	3300 ns	5000 ns
Tx/Rx (omni/horn) antenna	5/24 dBi or 2/19 dBi	2/19 dBi	2/19 dBi
Max. Tx-Rx distance	200 m	200 m	200 m
Tx/Rx height	2/2 m or 3/3 m	3/3 m	3/3 m

K. Haneda et al., EuCAP2016.



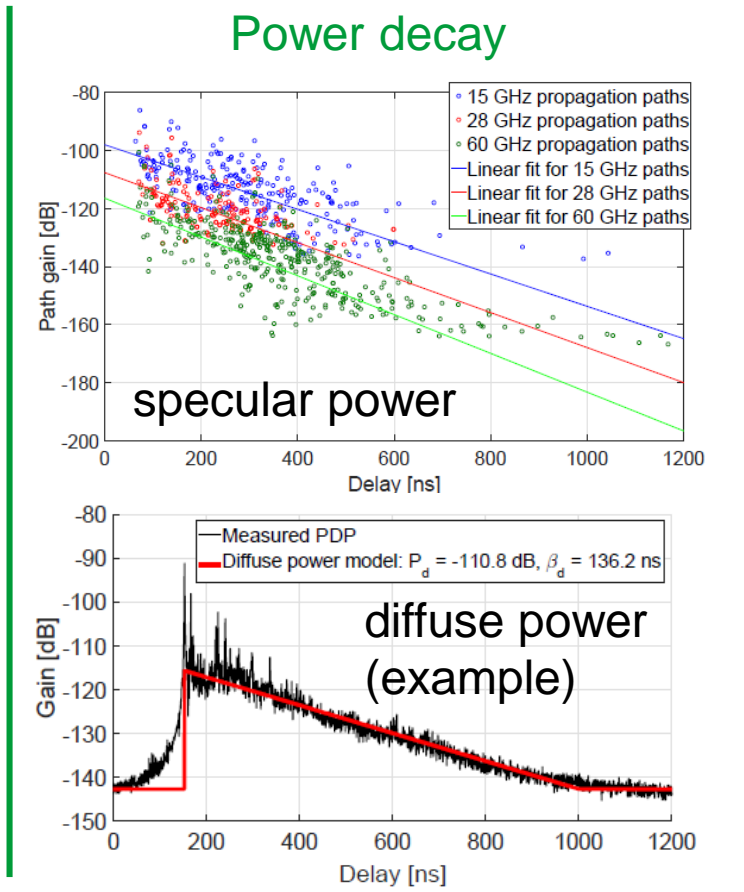
Multi-Frequency Channel Characterization in Helsinki

Airport



Mean large-scale parameters

	Frequency band	Delay spread [ns]	Azimuth spread [°]	Elevation spread [°]
	15 GHz	42.6	19.5	7.0
LOS	28 GHz	34.4	19.6	9.4
	60 GHz	38.7	17.6	5.6
	15 GHz	65.8	30.3	8.4
NLOS	28 GHz	N/A	N/A	N/A
	60 GHz	57.1	29.7	9.3



- Only slight frequency-dependence can be observed in the LSPs.
- Both specular and diffuse powers decay faster as frequency increases and specular power decays in general much faster than diffuse power.

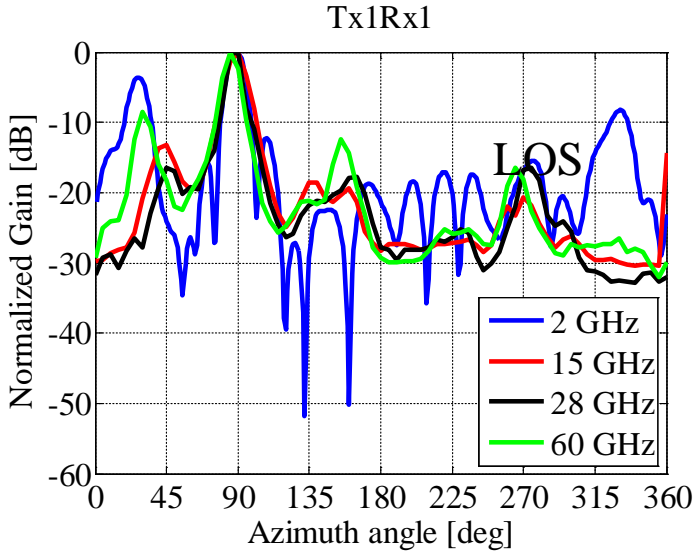


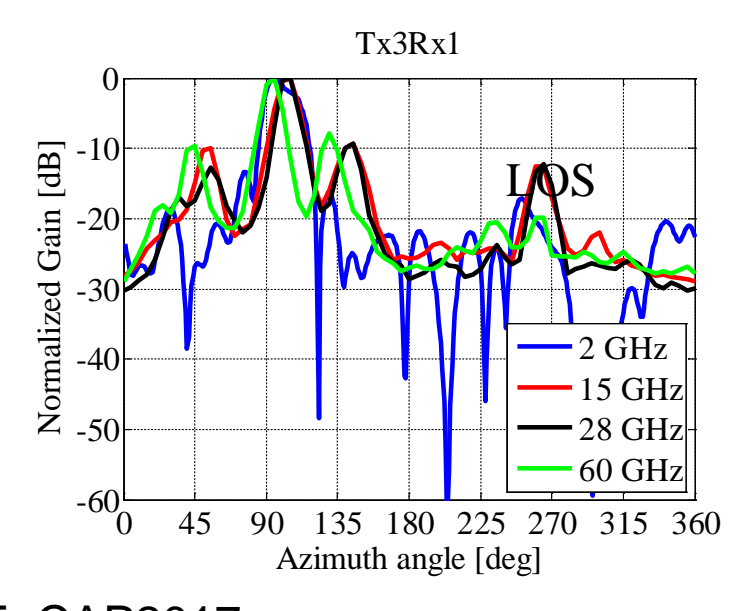
Comparison of Cm- and Mm-Wave Channels

PAS Comparison for indoor Environment at 2, 15, 28, 60 GHz



- Measurements based PAS evaluation at different frequencies
- PAS comparison below and above 6 GHz bands





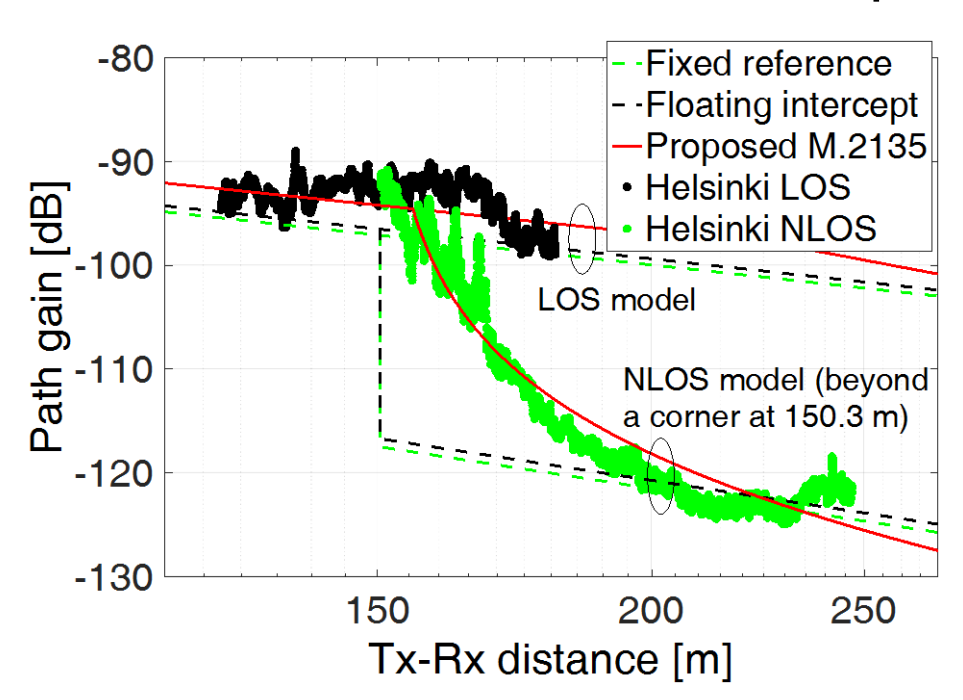


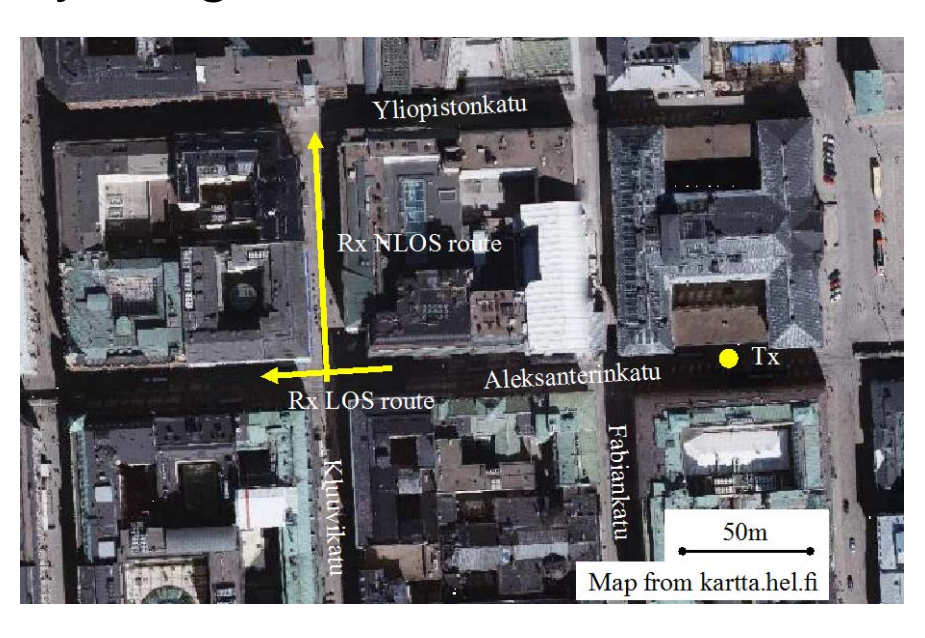
U.T. Virk, EuCAP2017 (won the best student paper award).

Frequency-Agile Pathloss Models



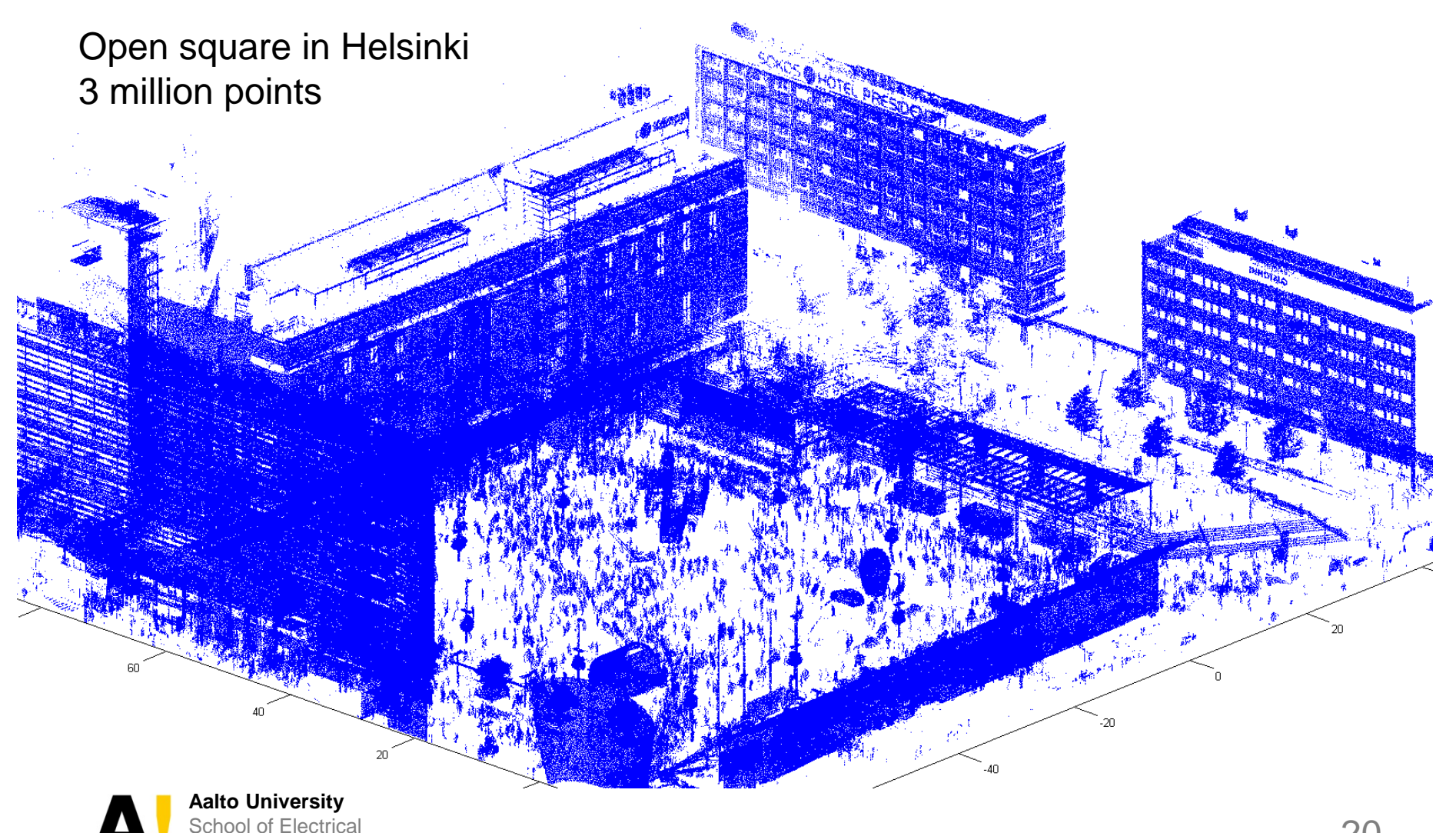
 Derived from channel sounding in urban street canyons of three cities for the frequency range of 0.8-60.4 GHz





- Models with varying complexity and accuracy parameterized
 - 1. Fixed reference model (wrt free-space loss at 1m)
 - 2. Floating intercept model (like ITU-R Hexagonal cell model)
 - 3. Modified ITU-R M.2135 two-ray model (LOS) and Manhattan grid model (NLOS)

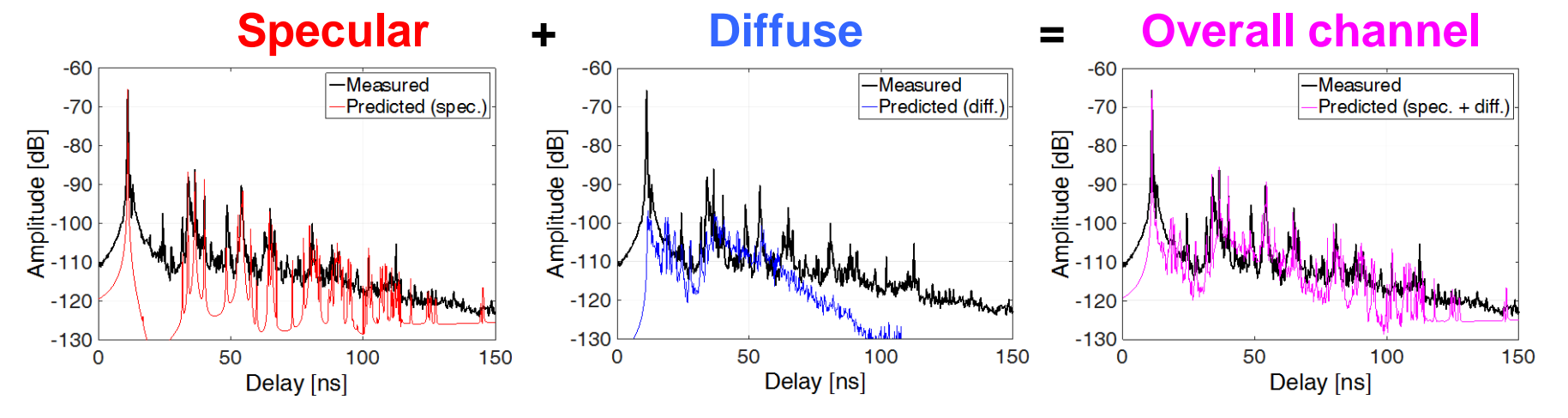
High Frequency Channel Simulations Using Optical Measurements of the Environment



Engineering

High Frequency Channel Simulations

- Points in the point cloud produce
 - Specular reflections
 - Diffuse scattering
 - Attenuation loss due to shadowing
- Material parameters (e.g. permittivity)
 optimized to fit measured channel impulse
 responses



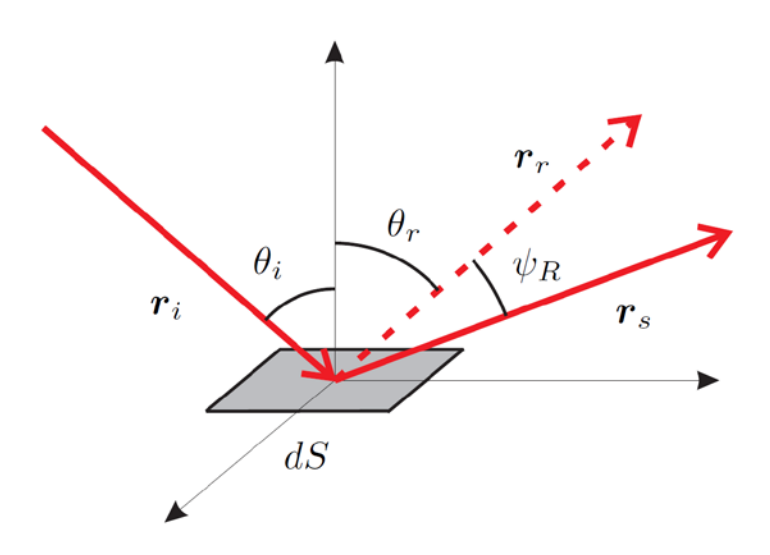


Street canyon @

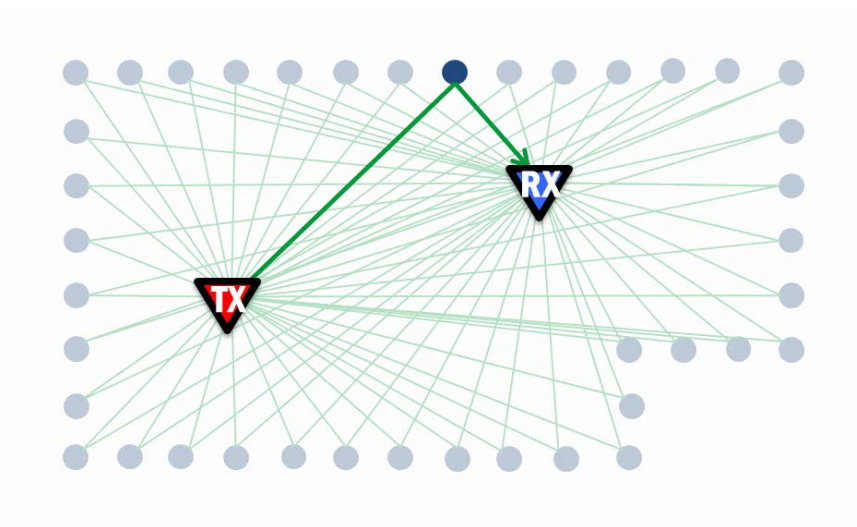
Aalto University

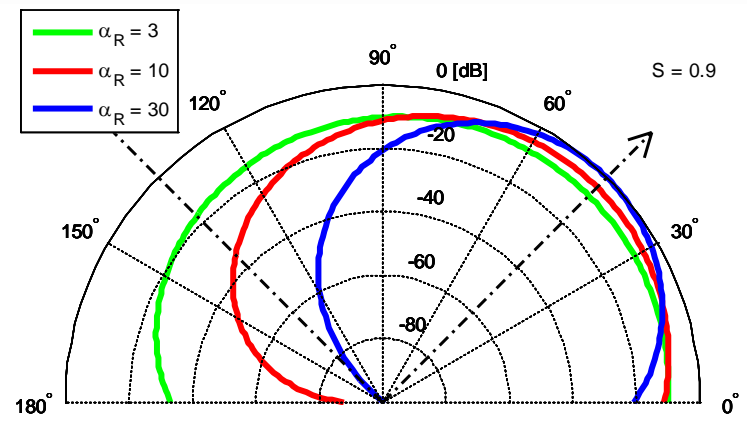
Diffuse Scattering Model

- Optimization on top of the specular components
- Scattering from each point calculated with single-lobe directive model [1]
- Material-dependent parameters S and α_R tuned based on measurements



$$\frac{P_r}{P_t} = \left\{ \left(\frac{S}{r_i r_s} \right)^2 \cdot \frac{dS \cos \theta_i}{F_{\alpha_R}} \right\} \cdot \left(\frac{1 + \cos \psi_R}{2} \right)^{\alpha_R} \cdot \left(\frac{\lambda}{4\pi} \right)^2$$



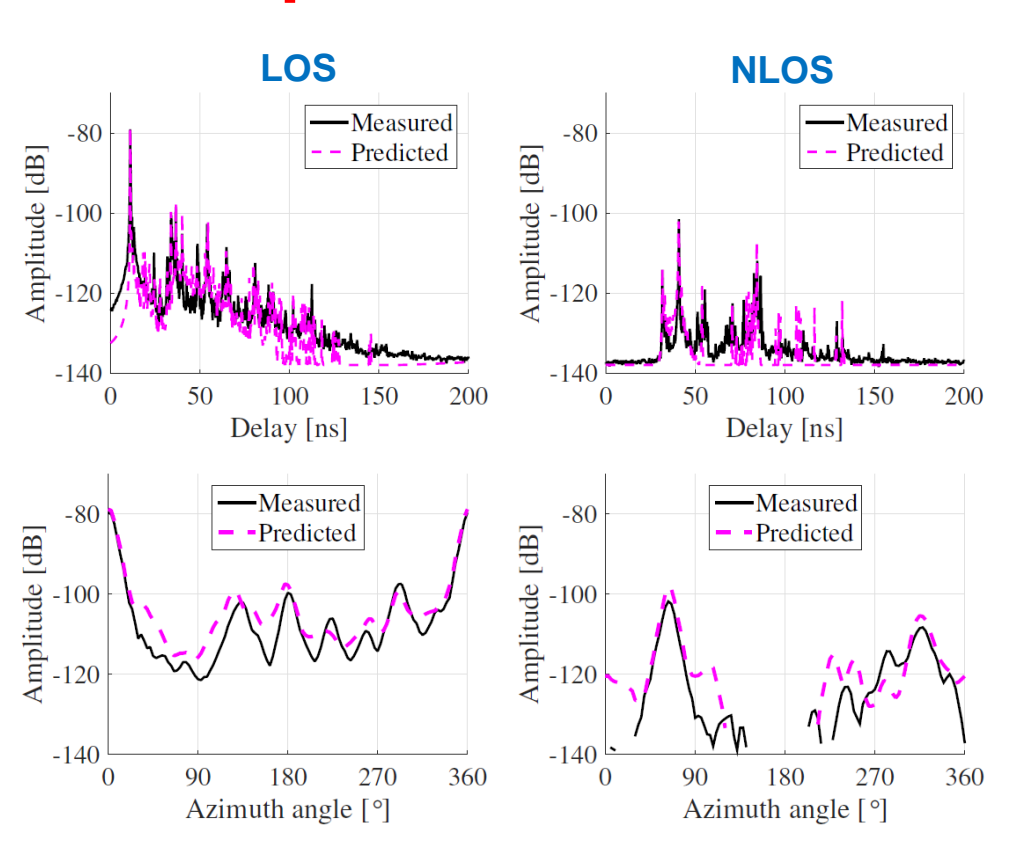


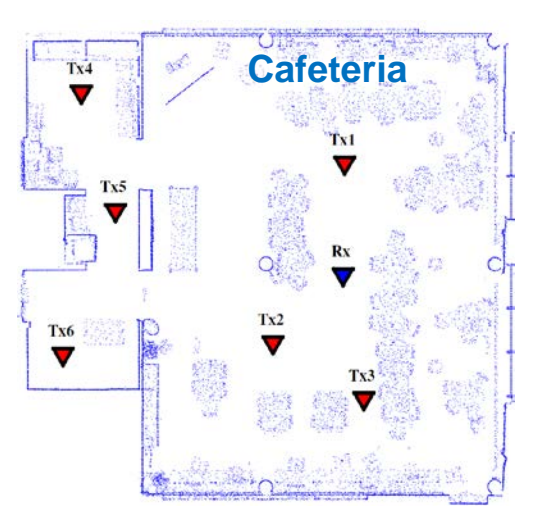
Higher $\alpha_R \rightarrow$ more directive scattering



[1] V. Degli-Esposti, et al., "Measurement and modelling of scattering from buildings," IEEE Trans. Ant. Prop., vol.55, no.1, pp.143-153, Jan. 2007.

Example: Indoor 60 GHz Channels



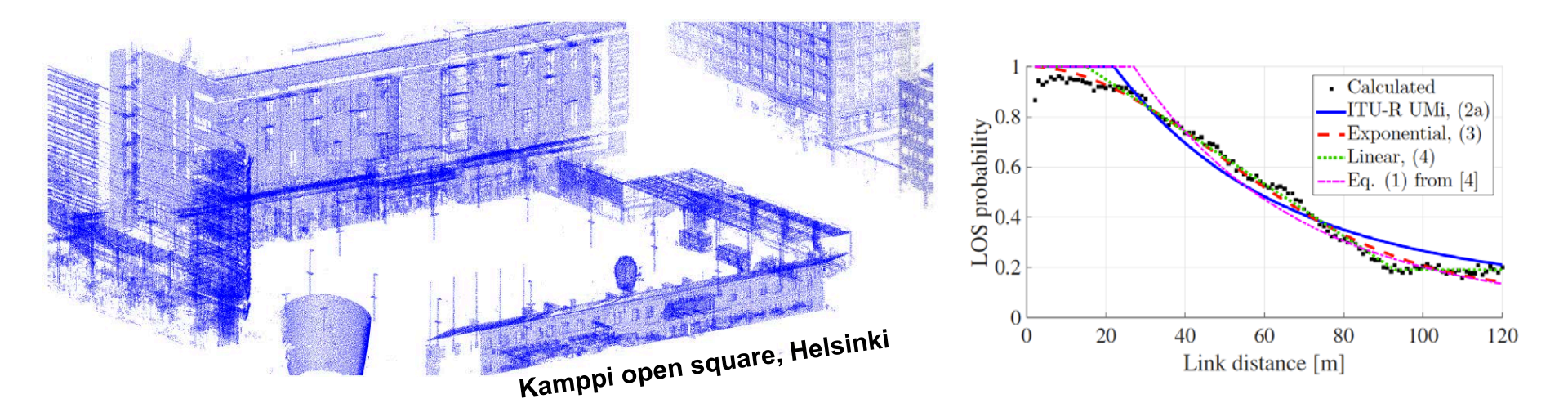


Link Tx		PL [dB]		$ au_{ m m}$ [ns]		$ au_{ m rms}$	$ au_{ m rms}$ [ns]		S_{ϕ} [°]	
\mathbf{type}	1 X	m.	р.	m.	р.	m.	р.	m.	р.	
ros	1	78.0	78.4	11.9	12.1	5.1	5.6	16.8	19.5	
	2	77.4	78.7	11.1	11.1	6.9	6.9	14.0	19.5	
	3	79.1	80.4	14.3	14.1	7.7	7.3	20.2	22.0	
NLOS	4	98.8	97.3	50.3	48.2	18.4	18.1	44.5	41.7	
	5	98.9	96.6	52.2	46.6	14.4	10.3	32.3	27.0	
Z	6	97.1	98.5	53.6	59.1	11.3	22.7	38.7	44.0	

- All relevant propagation mechanisms considered
 - Specular reflections, scattering, diffraction, shadowing
- Common indoor materials can be modeled with a single permittivity value
- Very good prediction accuracy in both LOS and NLOS conditions



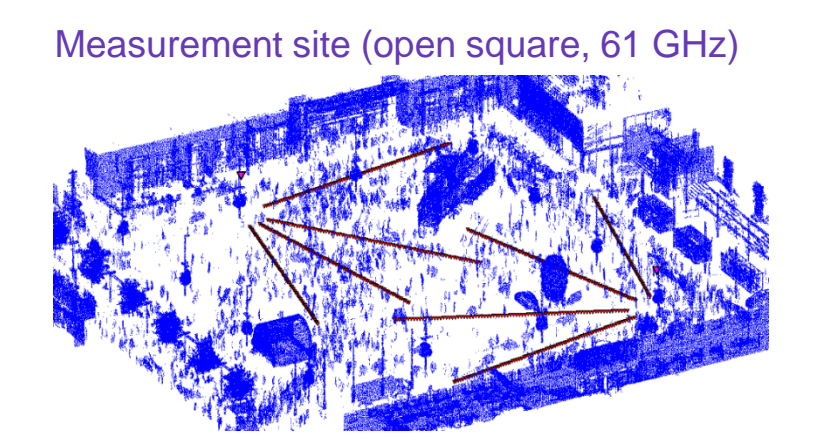
Mm-Wave Line-of-Sight Probability Evaluation Using Point Clouds

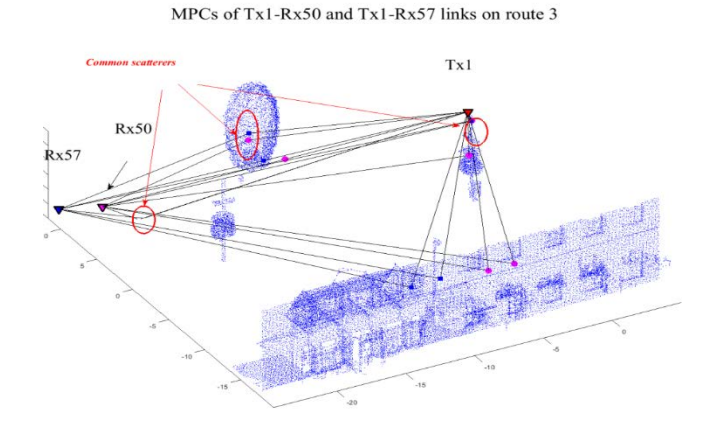


- Accurate description of environment allows very realistic modeling
- Fresnel zones used for shadowing detection → frequency dependent
- 3 scenarios: Open square, shopping mall, office
 - J. Järveläinen et al., IEEE Wireless Commun. Lett., 2016.

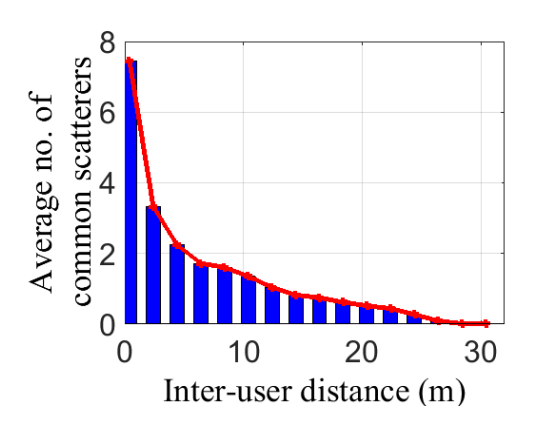


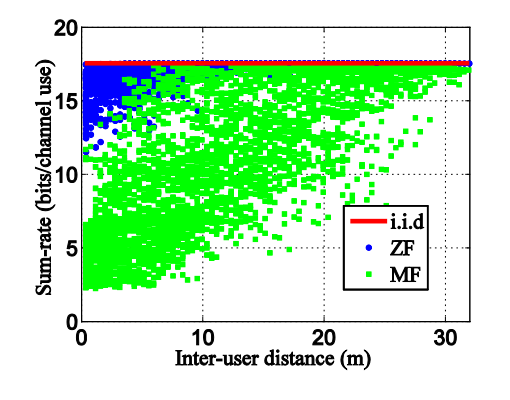
Orthogonality of Mm-Wave MU-MIMO Channels

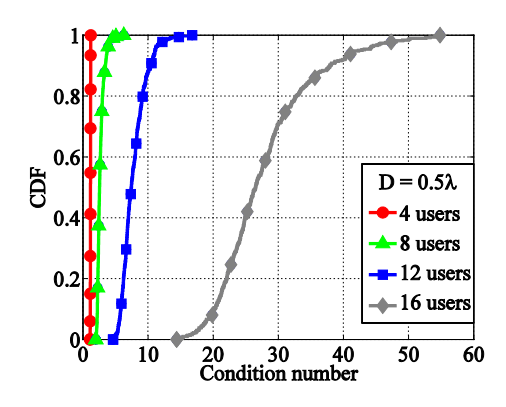




- Sparse multipaths, some scatterers are visible for multiple sites and users → Inter-link correlation
- When inter-user distance > twice of shadowing correlation distance, the average sum-rate of MF achieve 80% of i.i.d. sum-capacity







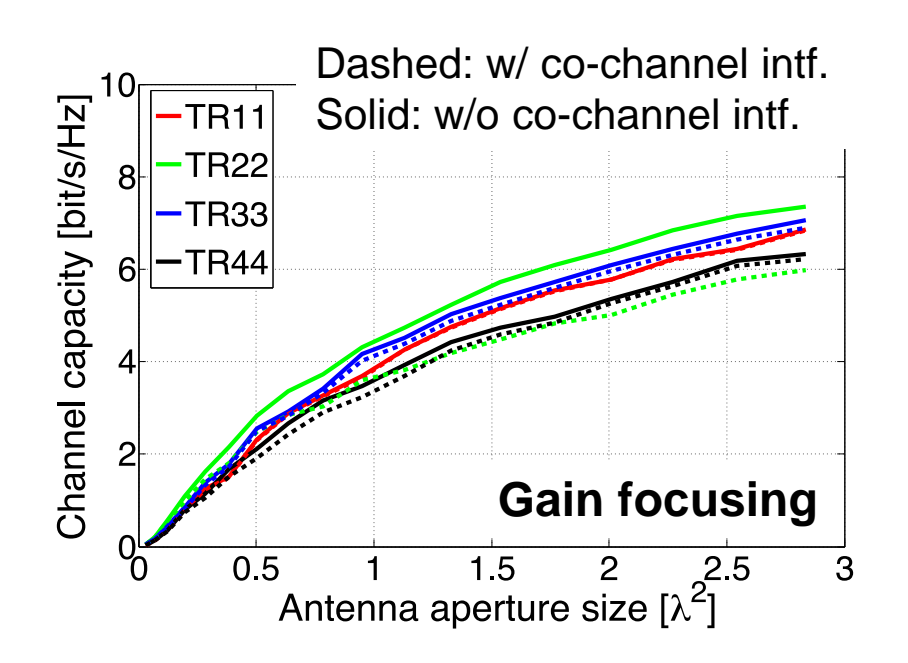


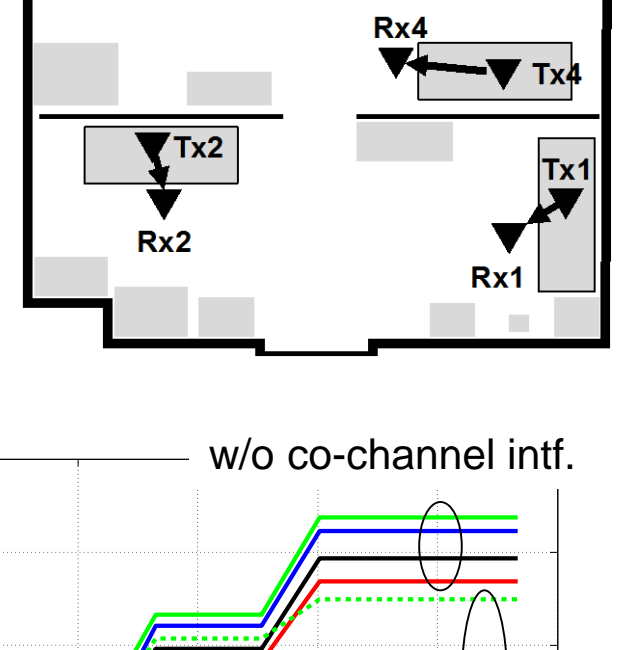
S. Nguyen et al., VTC Spring 2015.

Multi-User and Distributed Channels at Millimeter-Wave

- Example: coexistence analysis of distributed channels using point cloud channel simulations at 60 GHz
 - Revealed that single-mode beam focusing works as robust as eigenbeamforming.

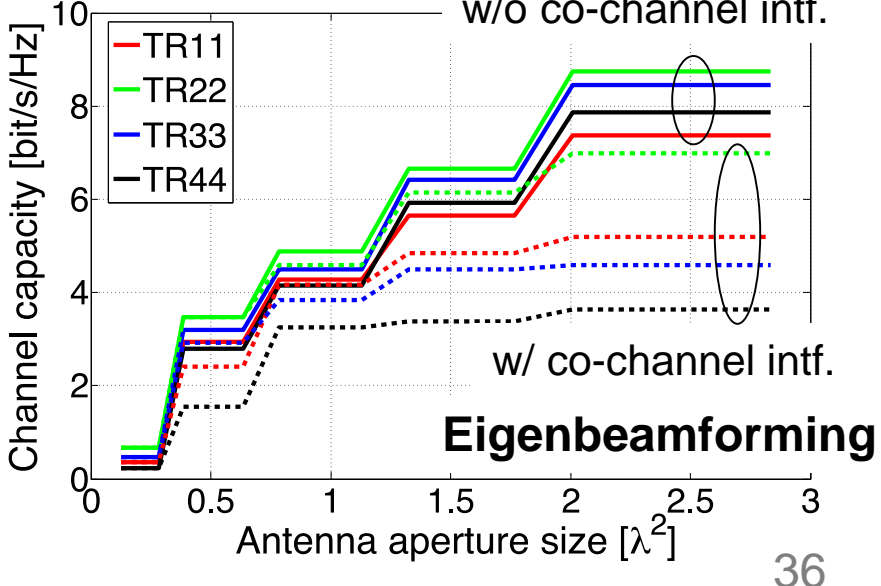
Haneda et al., VTC-Spring 2015.





Simulated

indoor room



Tx3

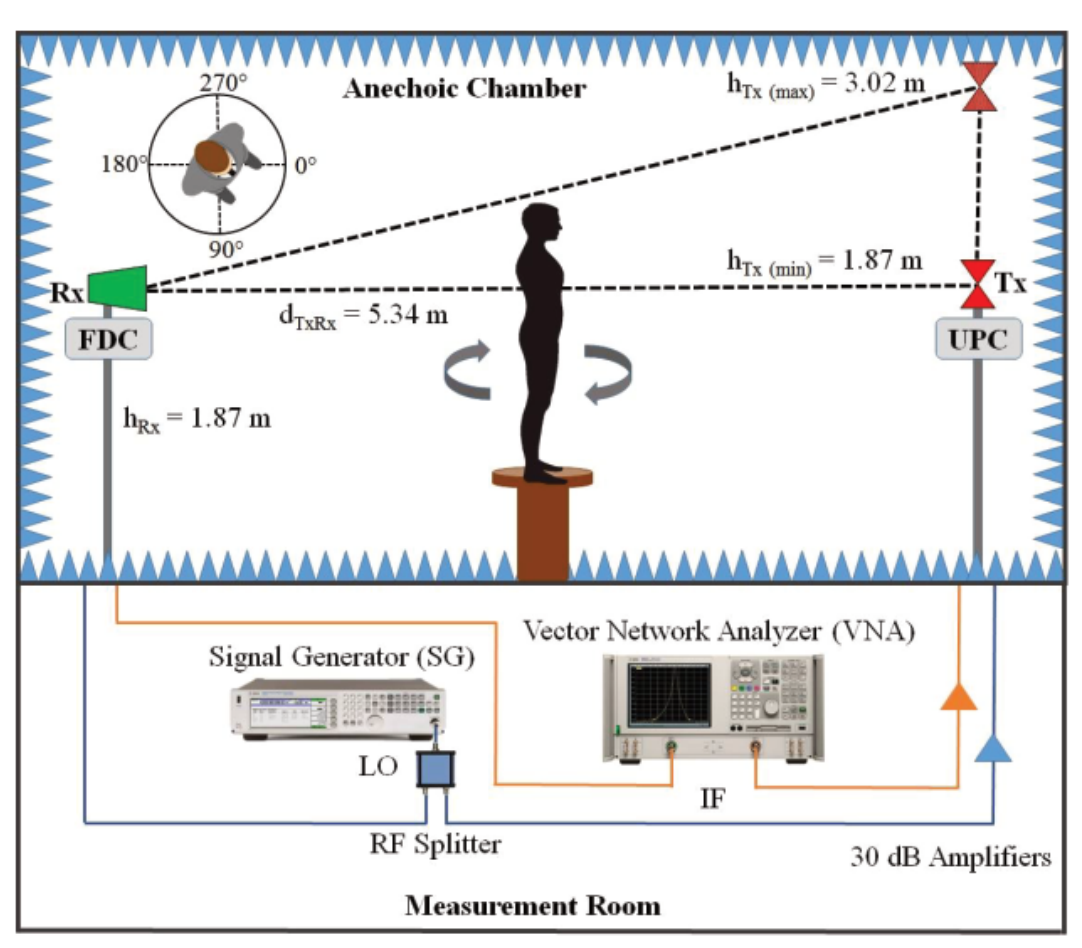
Rx3

Human-Channel Interaction

Far-field blockage is more noticeable at higher frequency

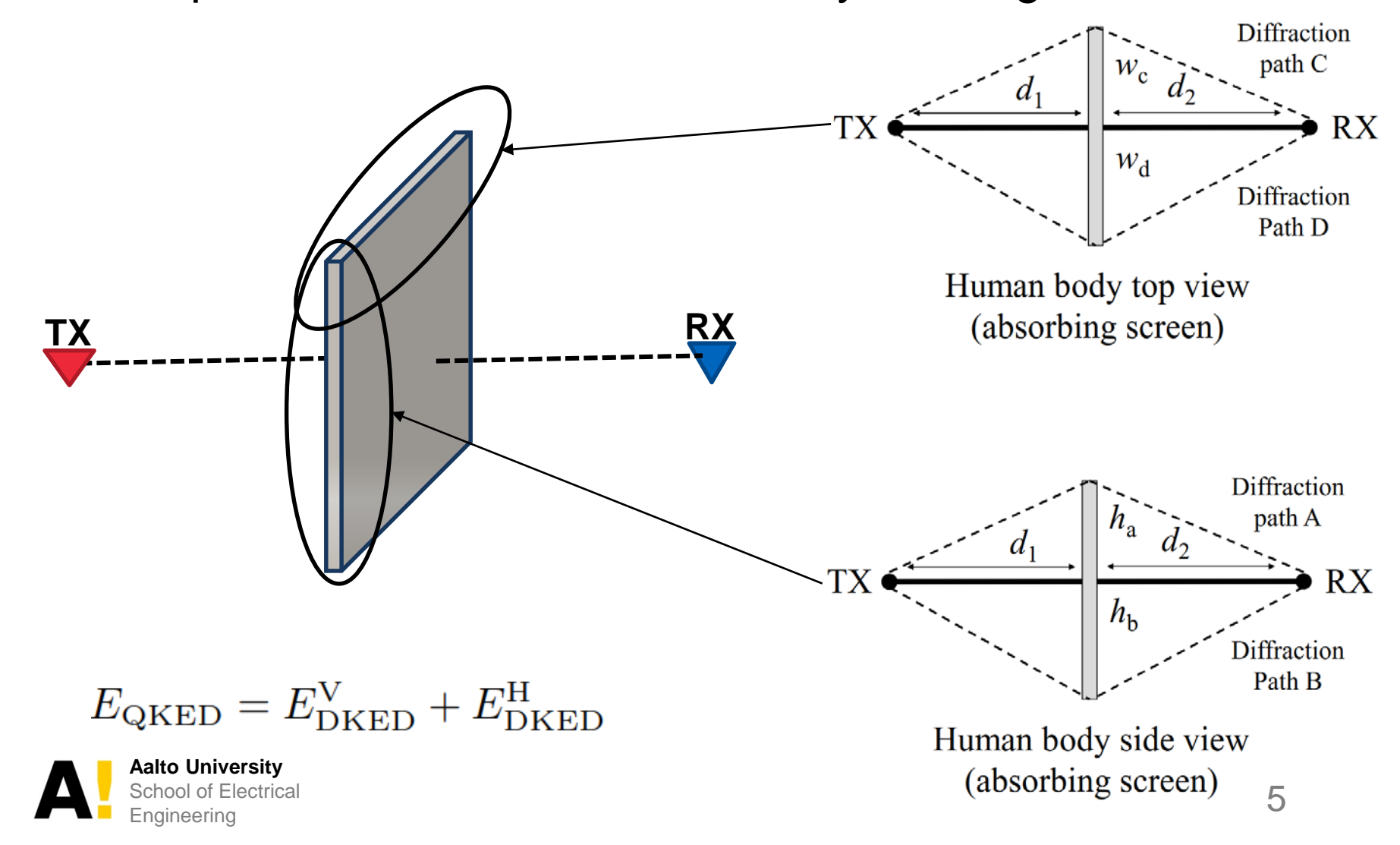
Measurements of 15 human body samples





Human-Channel Interaction

A simple model to calculate the body blockage loss

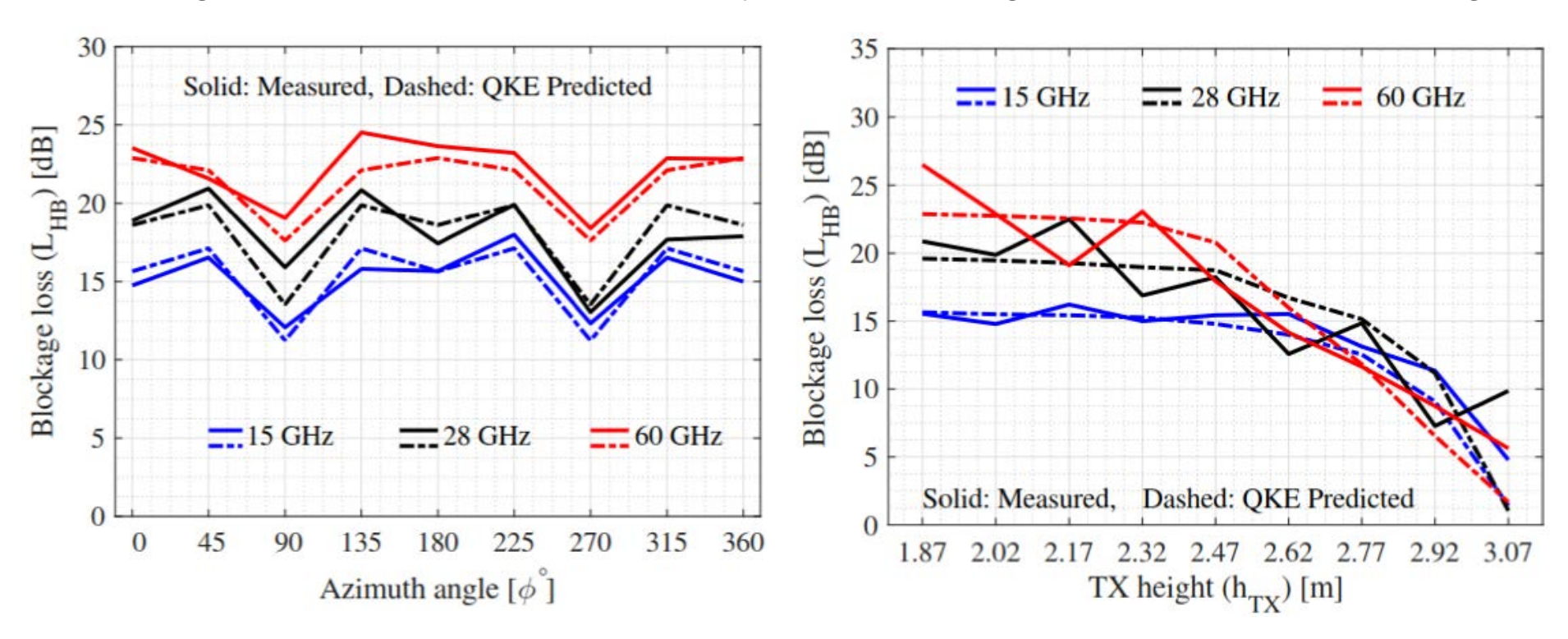


Human-Channel Interaction

Far-field blockage is more noticeable at higher frequency

Blockage vs Orientation of human body

Blockage vs transmit antenna height

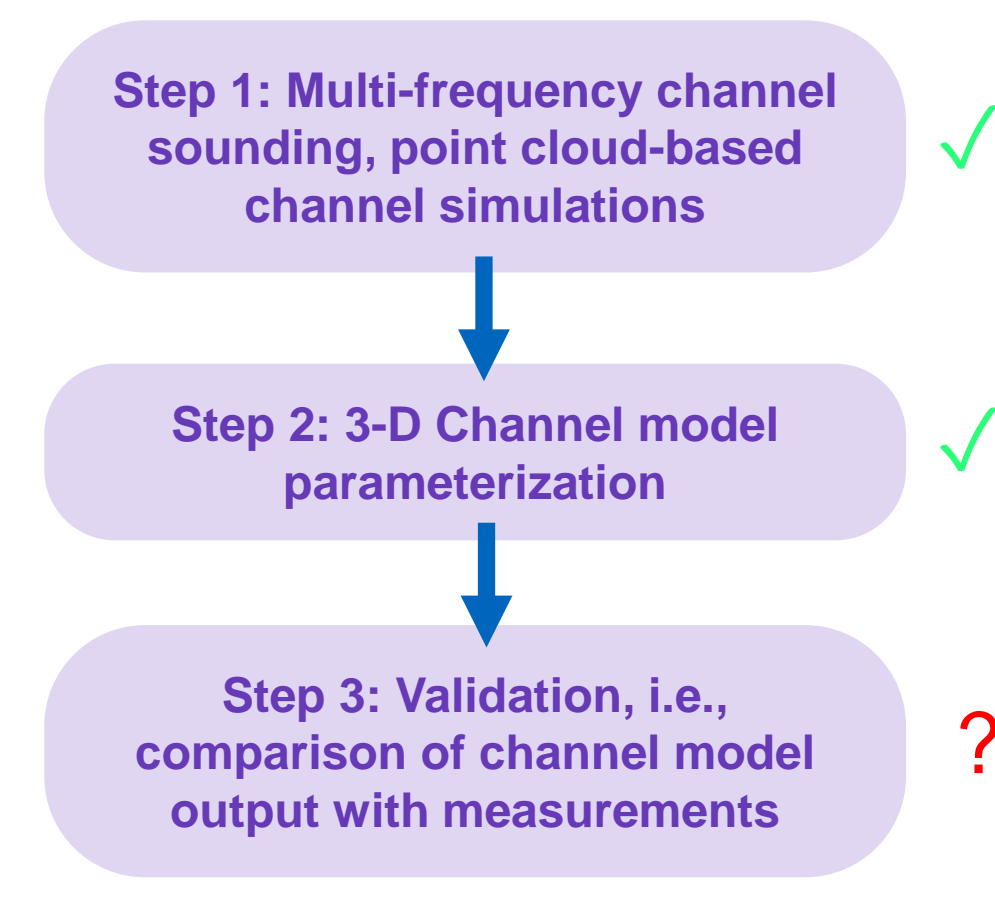


We made a model that reproduces median blockage losses over 15 body samples



Does a GSCM Reproduce the Reality?

 Validation of small-scale fading characteristics for a stochastic channel model (WINNER in our case)



Comparison does not always go well ⊗

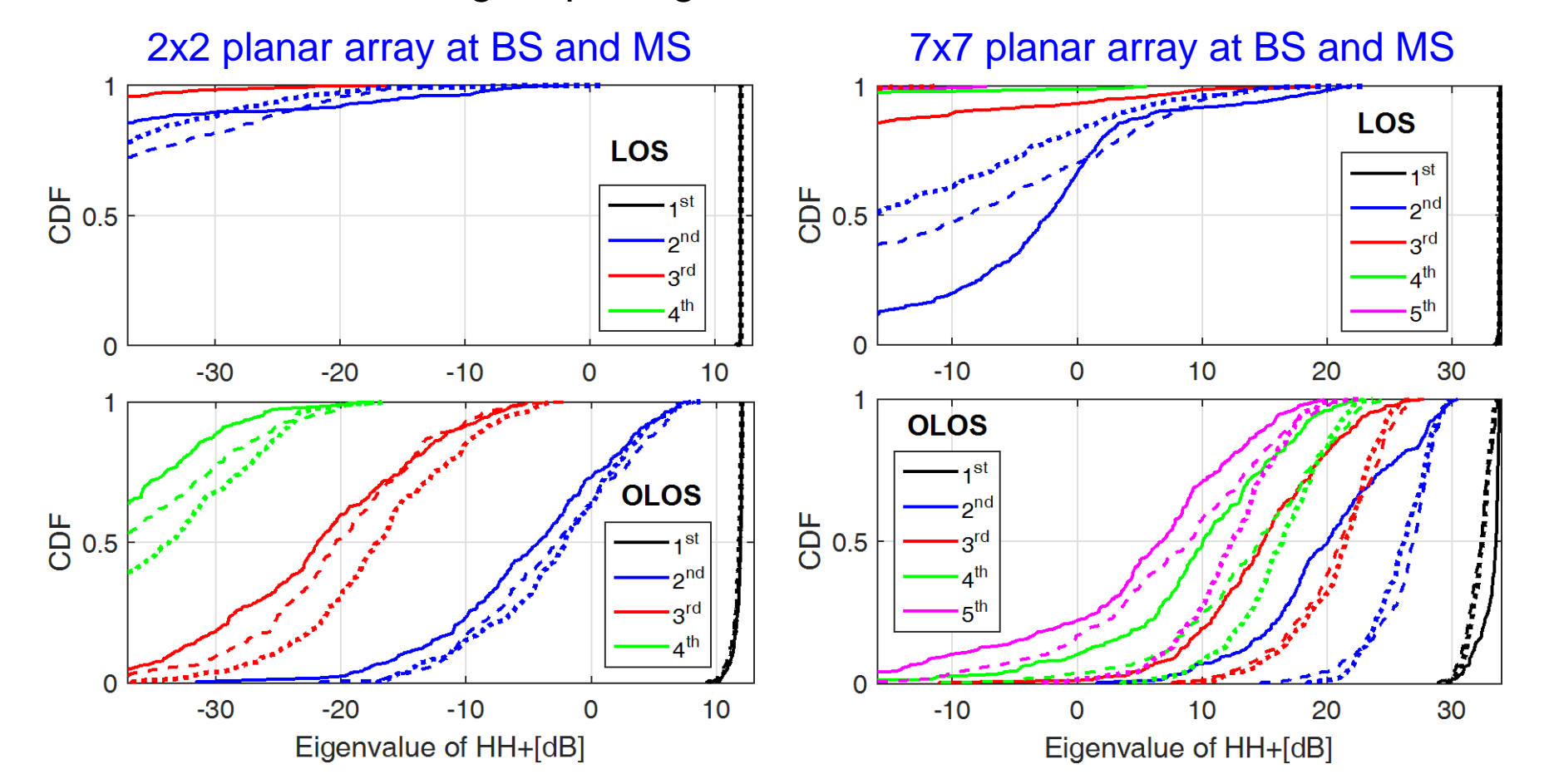
- Angular and delay spreads
- # of clusters and
 sub-paths
- √ Max excess delay
- X Eigenvalue distributions of MIMO channels with large antenna array



Eigenvalue Distributions of MIMO Channels

- Array configurations at the BS and MS:
 - The same uniform horizontal planar array
 - Half-wavelength dipole antennas
 - Half-wavelength spacing btw antennas

Solid lines: point cloud Dashed lines: WINNER (1 or 20 rays)



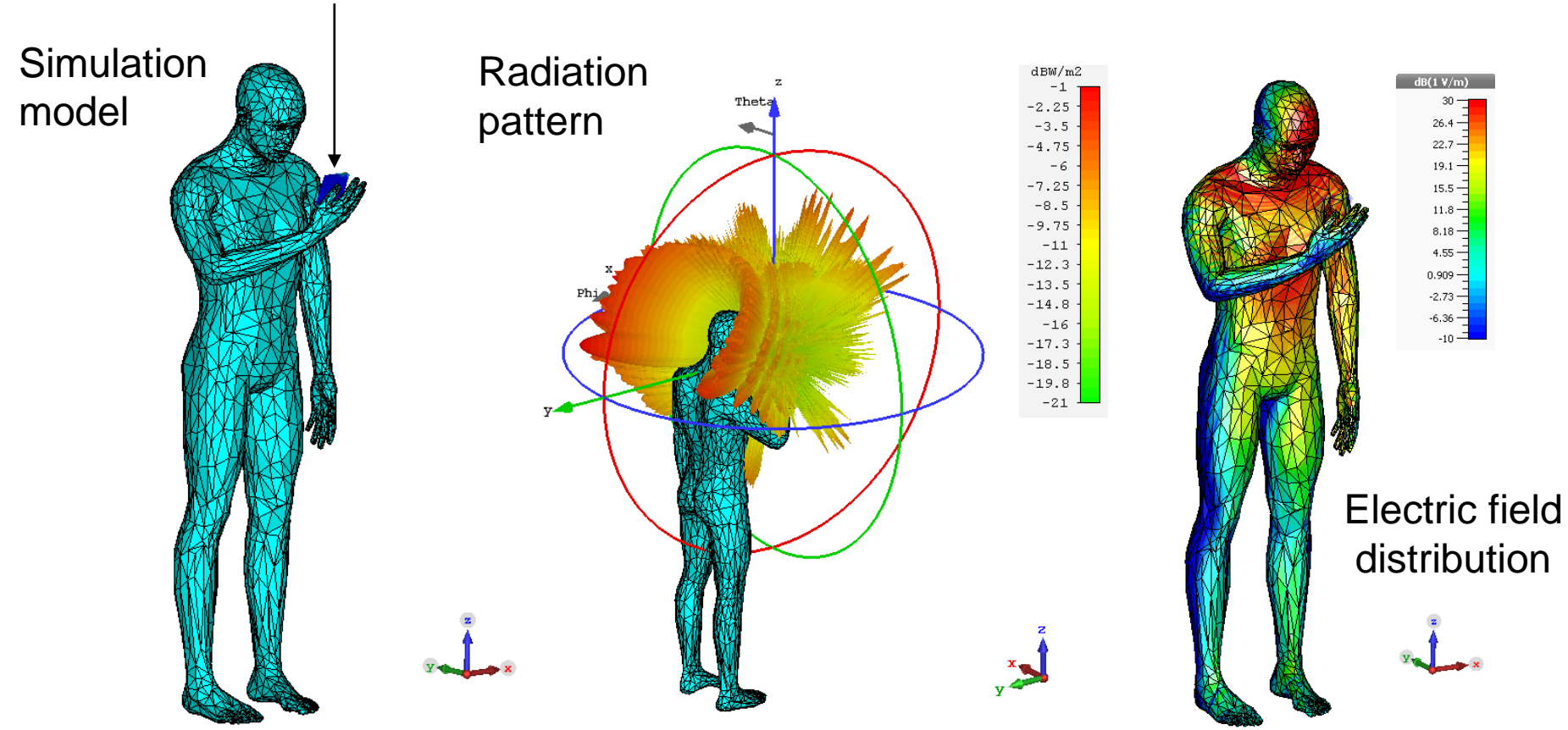
Over-the-Air Antenna Test Methods



Antenna-Human Interaction

Also more noticeable self-body blockage effects

A patch antenna on a mobile phone-sized ground plane

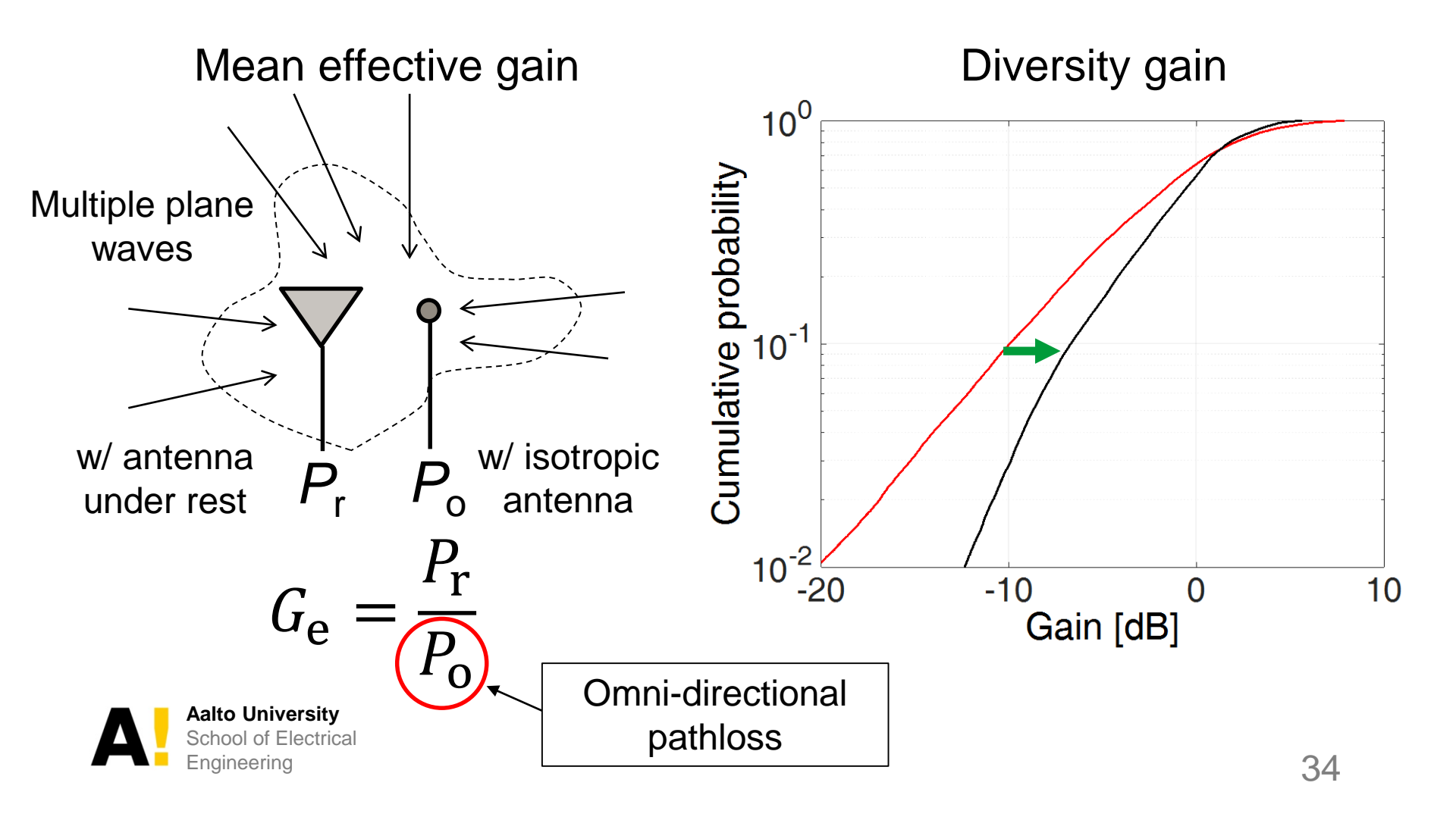




Figures-of-Merit

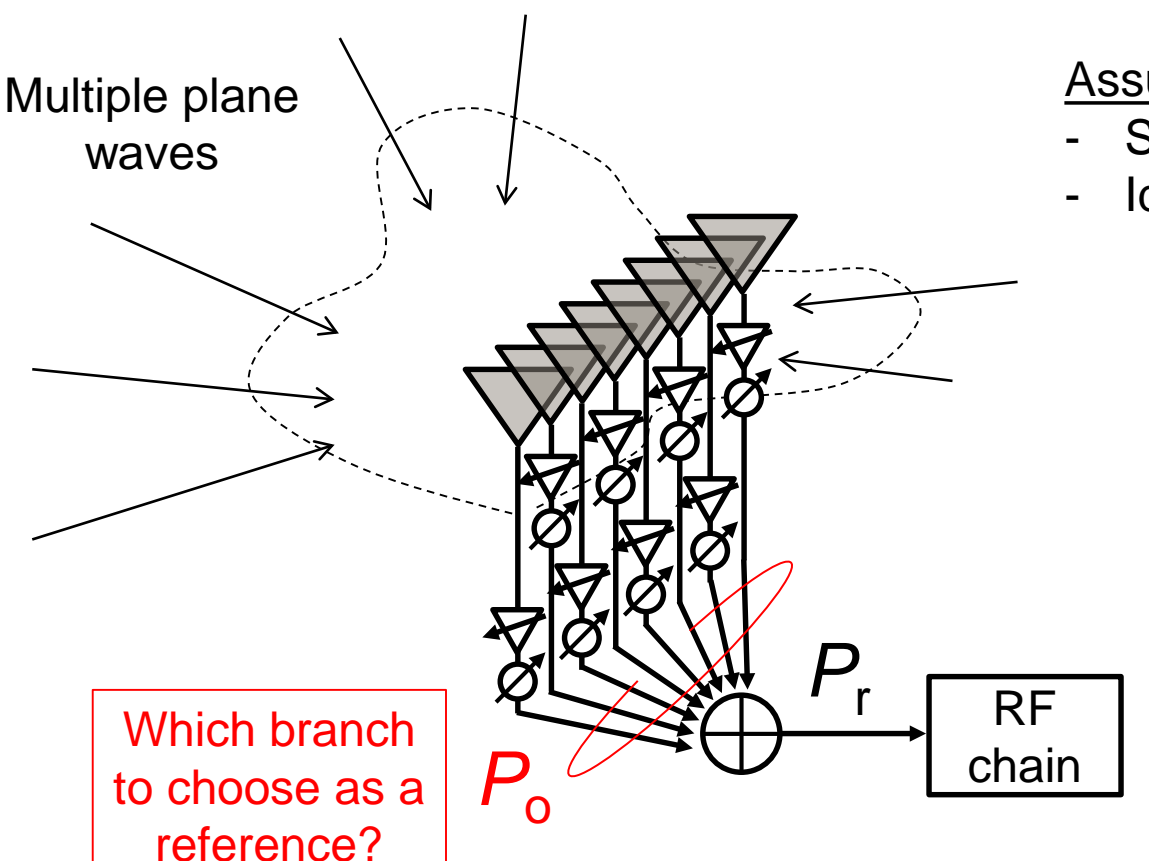
Vaughan and Andersen, TVT, 1987. Taga, TVT, 1990.

 Evaluation metrics of a mobile phone antenna element and array in an operational (multipath) environment



Array Gain

 An evaluation metric of a mobile phone antenna element and array in an operational (multipath) environment



Assumptions in our study:

- Single RF chain
- Ideal maximum-ratio combining

$$G_{\mathrm{e}} = \frac{P_{\mathrm{r}}}{P_{\mathrm{o}}}$$

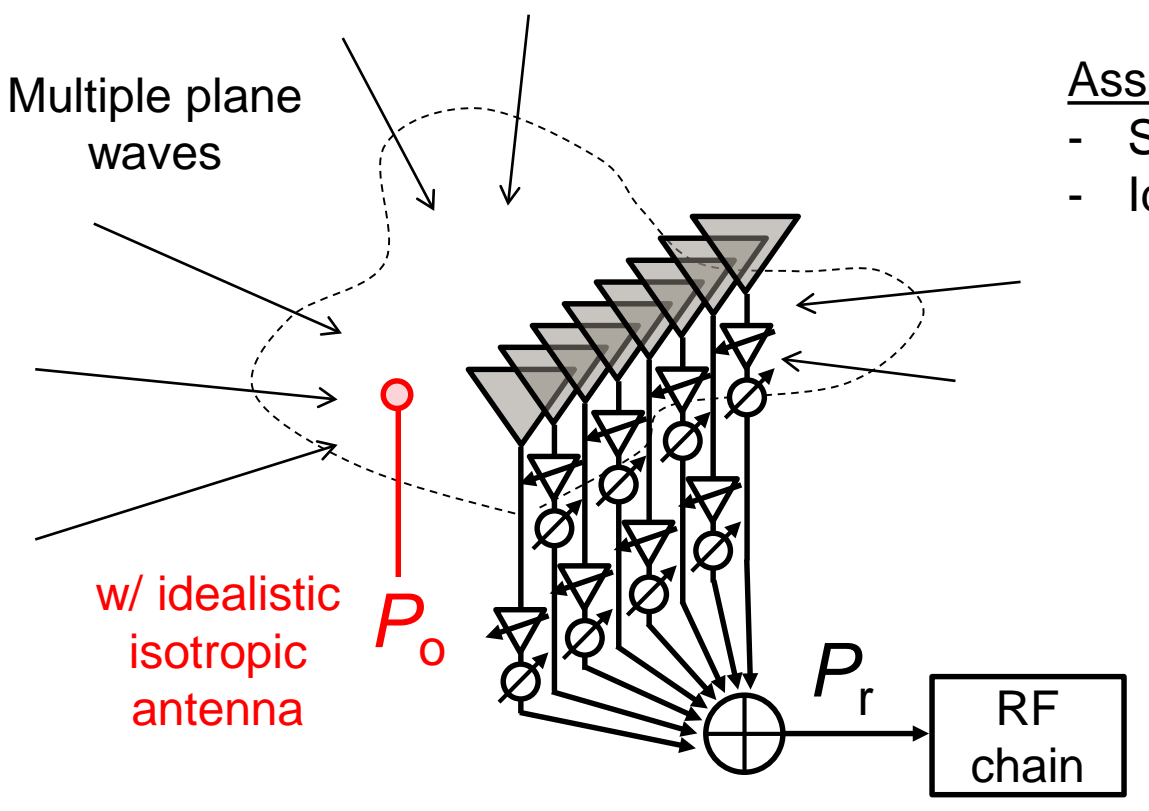
Gain may be different, depending on a chosen reference branch.

Aalto University
School of Electrical
Engineering

Vaughan and Andersen, Channels, Propagation and Antennas for Mobile Communications, IEE Electromagnetic Series 50, 2003.

Total Array Gain

 An evaluation metric of a mobile phone antenna array in an operational (multipath) environment



Assumptions in our study:

- Single RF chain
- Ideal maximum-ratio combining

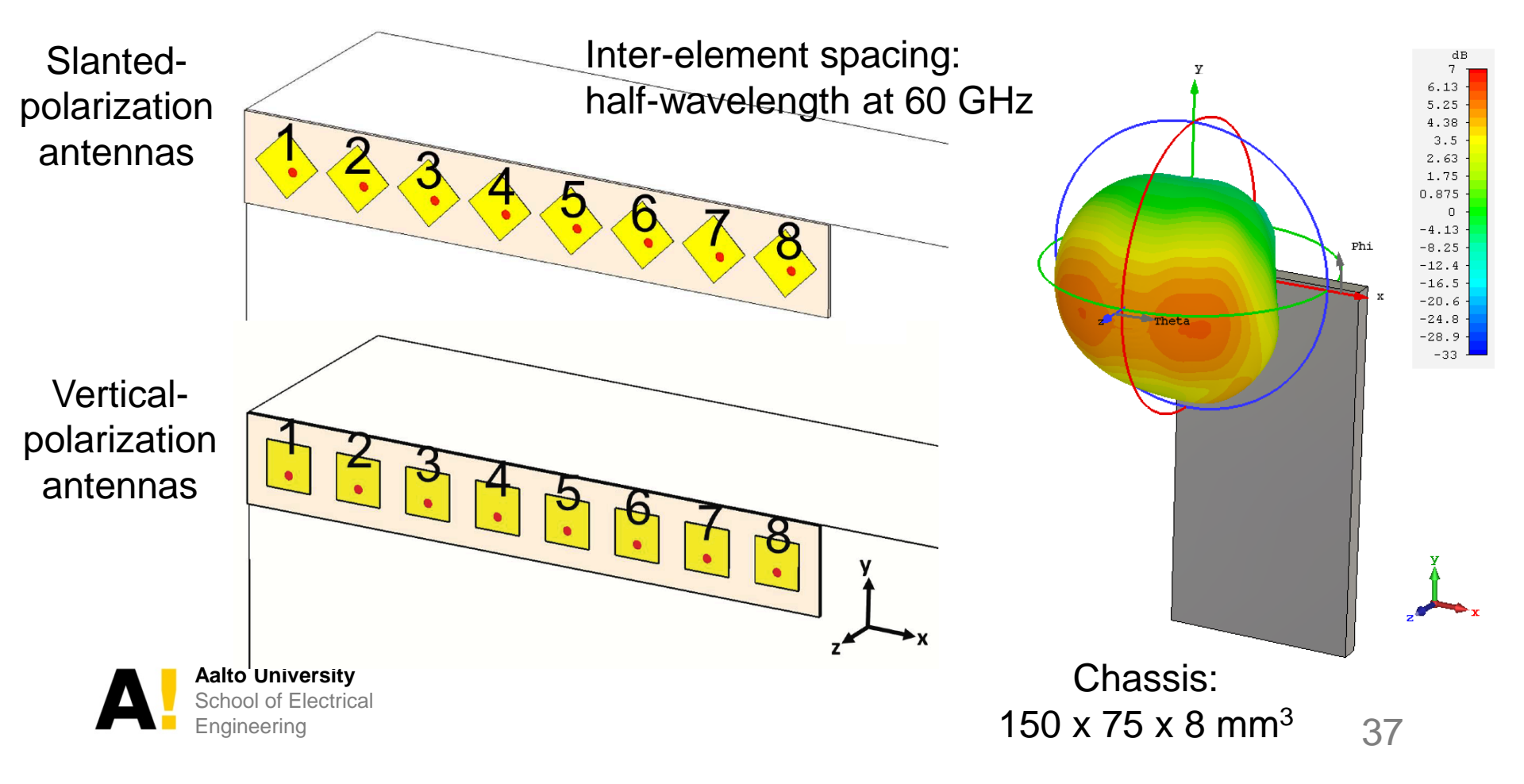
$$G_{\mathrm{e}} = \frac{P_{\mathrm{r}}}{P_{\mathrm{o}}}$$

Gain is uniquely defined, regardless of branch power imbalance.



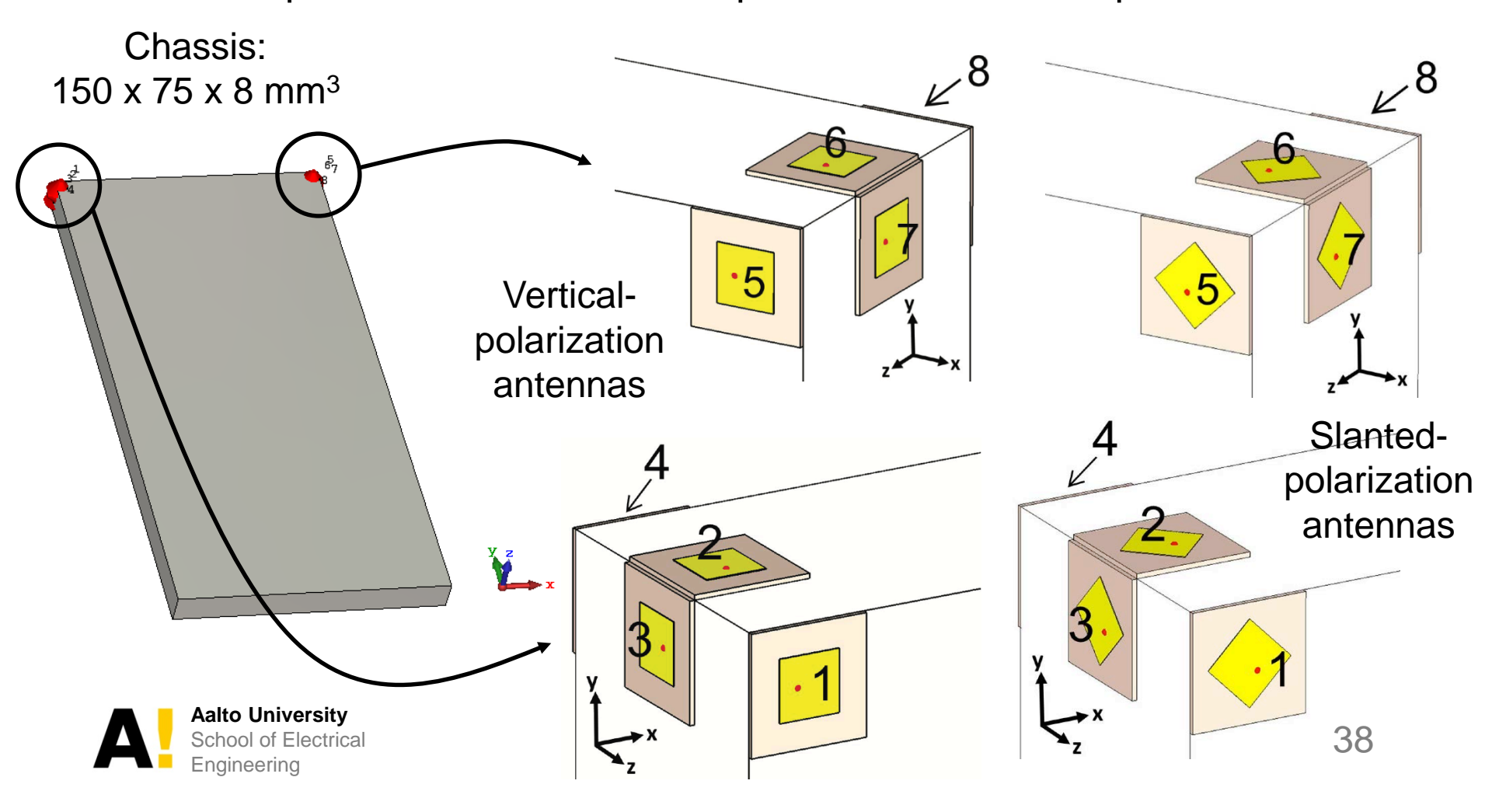
Mobile Phone Antenna Arrays at 60 GHz (1)

- Uniform antenna array (ULA)
 - Eight patch antennas at a corner of a smart phone, radiating slanted polarization to the ground at a vertical posture of a phone

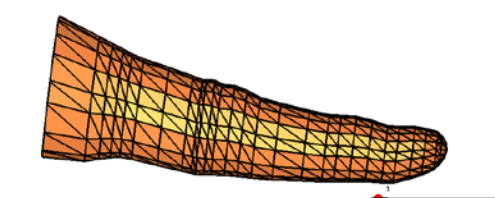


Mobile Phone Antenna Arrays at 60 GHz (2)

- Distributed array (DA)
 - Four patch antennas at two top corners of a smart phone

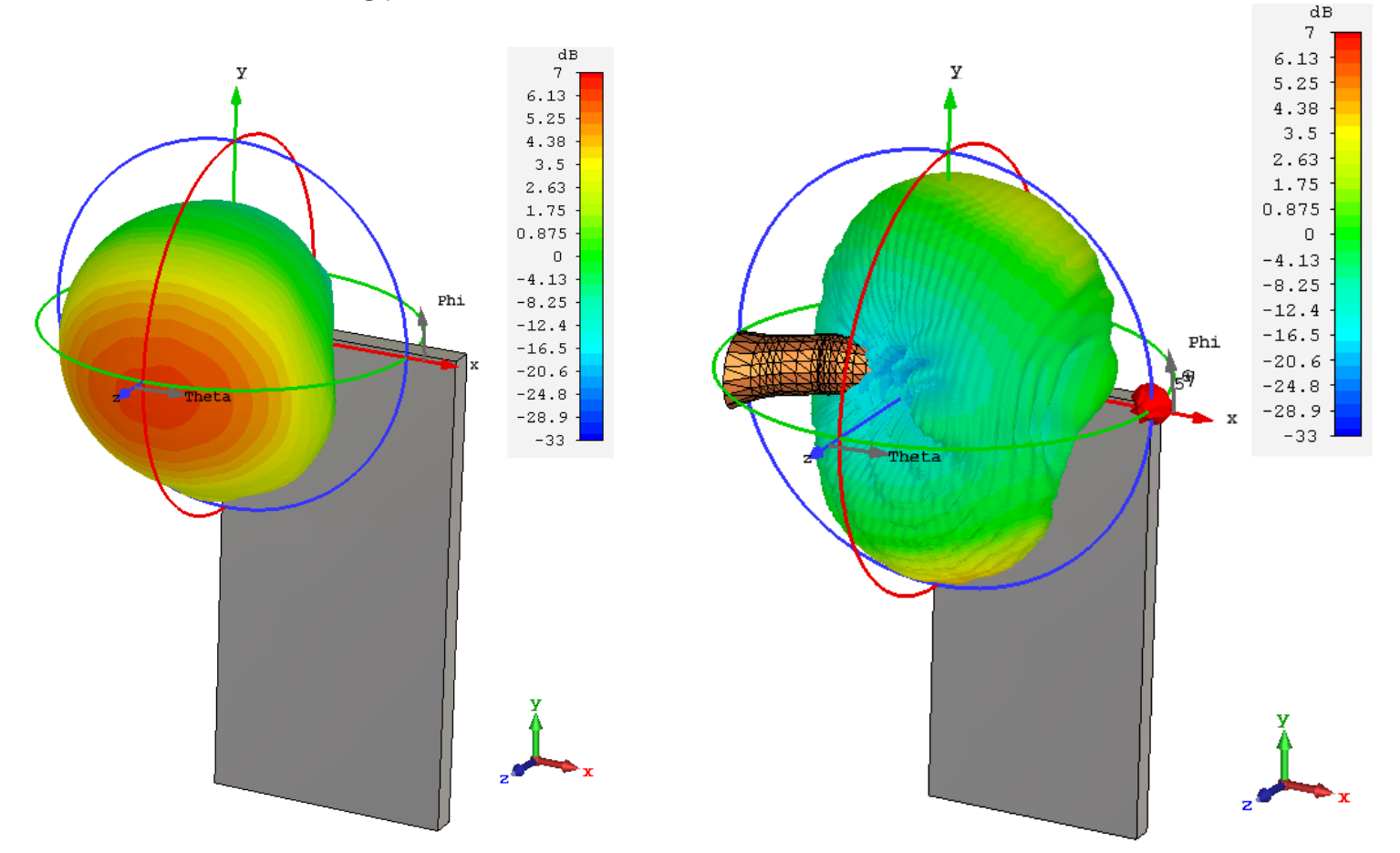


Finger Effects





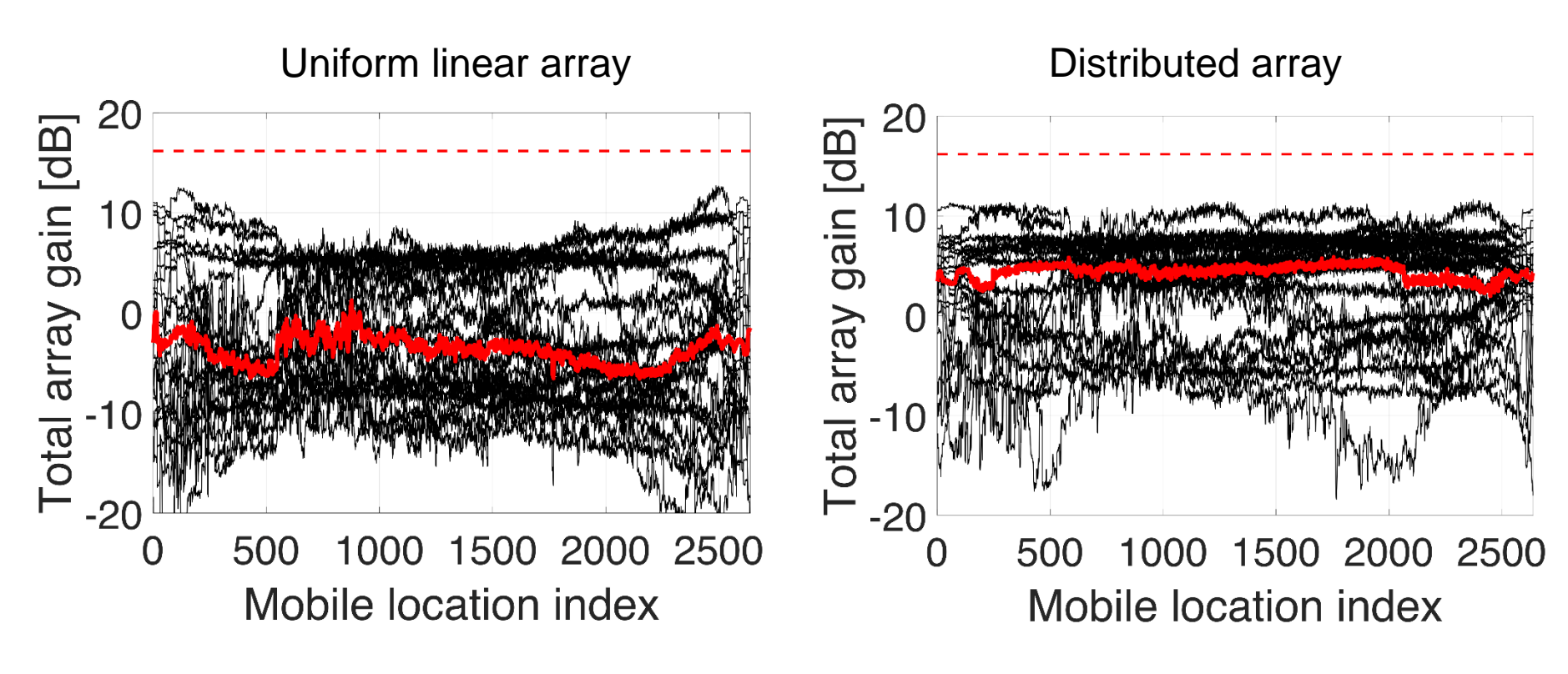
 20 dB reduction of the broadside gain at 60 GHz; more energy spread to other directions





Total Array Gain Uniform linear array (ULA) vs. distributed array (DA)

DA outperforms ULA in the total array gain and capacity.



BS: single dual-pol omni-antenna, MS: Maximum radio combining



- Tutorials, invited talks and magazine articles
 - K. Kusume et al., "Radio propagation modeling for 5G mobile and wireless communications," IEEE Communications Magazine, vol. 54, no. 6, pp. 144-151, June 2016.
 - K. Haneda, "Millimeter-Wave Propagation and Channel Measurements What is done and what is undone," Session panelist of the EuCAP2016 Workshop on key enabling technologies on antenna and channel models for an effective mmWave 5G deployment, April 2016.
 - K. Witrisal et al., "High-accuracy localization for assisted living: 5G systems will turn multipath channels from foe to friend," IEEE Signal Processing Magazine, vol. 33, no. 2, pp. 59–70, March 2016.
 - K. Haneda, "Channel models and beamforming at millimeter-wave frequency bands," IEICE Transactions on Communications, vol. E98-B, no. 5, May 2015 (won the best tutorial paper award).
 - M. Heino et al., "Recent advances in antenna design and interference cancellation algorithms for in-band full-duplex relays," IEEE Commun. Mag., vol, 53, no. 5, pp. 91–101, May 2015.
 - K. Haneda, "Channel model: 5G air interface," Session panelist of the Brooklyn 5G
 Aalto University So Summer in New York, April 2015.

- Antennas and antenna measurements (selected papers)
 - K. Iwamoto et al. "Design of an antenna decoupling scatterer for an inband full-duplex collinear dipole array," IEEE Trans. Ant. Prop., vol. 66, no. 7, pp. 3763-3768, July 2018.
 - S. Venkatasubramanian et al., "Impact of using resistive elements for wideband isolation improvement," IEEE Trans. Ant. Prop., vol. 65, no. 1, pp. 52-62, Jan. 2017.
 - L. Li et al., "Compact dual-band antenna array for massive MIMO," 27th Int. Symp.
 Personal, Indoor and Mobile Radio Commun., Valencia, Spain, Sep. 2016.
 - A. Khatun et al., "Experimental verification of a plane-wave field synthesis technique for MIMO OTA antenna testing," IEEE Trans. Ant. Prop., vol. 64, no. 7, pp. 3141– 3150, July 2016.
 - M. Heino et al., "Finger effect on 60 GHz user device antennas," 10th European Conference on Antennas and Propagation, Davos, Switzerland, April 2016.
 - M. Md. Suzan et al., "A conformal antenna for capsule endoscopy: Design, analysis, and experimental validation," 10th Euro. Conf. Ant. Prop., Davos, Switzerland, April 2016.
 - M. Heino et al., "Design of wavetraps for isolation improvement in compact in-band full-duplex relay antennas," IEEE Trans. Ant. Prop., vol. 64, no. 3, pp. 1061–1070, soMarch 2016.

42

- Channels and measurements (selected papers)
 - S. L. H. Nguyen et al., "On the frequency dependency of radio channel's delay spread: Analyses and findings from mmMAGIC multi-frequency channel sounding," 12th European Conf. Ant. Prop. (EuCAP 2018), London, UK, April 2018.
 - S. L. H. Nguyen et al., "Comparing radio propagation channels between 28 and 140 GHz bands in a shopping hall," 12th European Conf. Ant. Prop. (EuCAP 2018), London, UK, April 2018.
 - J. Jarvelainen, K. Haneda and A. Karttunen, "Indoor propagation channel simulations at 60 GHz using point cloud data," IEEE Trans. Ant. Prop., pp. 4457-4467, Aug. 2016.
 - K. Haneda, N. Omaki, T. Imai, L. Raschkowski, M. Peter and A. Roivainen,
 "Frequency-agile pathloss models in urban street canyons," IEEE Trans. Ant. Prop.,
 vol. 64, no. 5, pp. 1941–1951, May 2016.
 - S. Hur, S. Beak, B. Kim, Y. Chang, K. Haneda, A. F. Molisch, T. S. Rappaport and J. Park, "Proposal on mmWave Channel Modeling for 5G Cellular System," IEEE J. Sel. Areas Commun., vol. 10, no. 3, pp. 454-469, April 2016.
 - C. Gustafson, K. Haneda, S. Wyne, and F. Tufvesson, "On mm-wave multi-path clustering in a conference room environment," IEEE Transactions on Antennas and Propagation, vol. 62, no. 3, pp. 1445-1455, Mar. 2014.



- Systems (selected papers)
 - K. Haneda et al., "Total array gains of polarized millimeter-wave mobile phone antennas," 27th European Conf. Networks Commun. (EuCNC 2018), Ljubljana, Slovenia, June 2018.
 - A. F. Molisch et al., "Hybrid beamforming for massive MIMO a survey," IEEE
 Wireless Communications Magazine, vol. 55, no. 9, pp. 134-141, September 2017.
 - K. Haneda et al., "Attainable capacity of spatial channels: a multiple-frequency analysis," 2016 Global Commun. Conf. (Globecom'16) Workshop on Mobile Commun. for High Frequency Bands, Washington DC, Dec 2016.
 - J. Jarvelainen et al., "Evaluation of mm- wave line-of-sight probability with point cloud data," IEEE Wireless Commun. Lett., vol. 5, no. 3, pp. 228–231, June 2016.
 - S. L. H. Nguyen et al. "On the mutual orthogonality of millimeter-wave massive MIMO channels," 81st Vehicular Technology Conference (VTC2015-Spring), Glasgow, Scotland, May 2015.
 - K. Haneda et al., "Spatial coexistence of millimtre-wave radio links in an indoor environment," 81st Vehicular Technology Conference (VTC2015- Spring), Glasgow, Scotland, May 2015.

